PB81-234114

Environmental Effects of Pollutants from Coal Combustion 2. The Colstrip, Montana Power Plant

(U.S.) National Oceanic and Atmospheric Administration, Boulder, CO

Prepared for

Environmental Protection Agency
Washington, DC

Apr 81

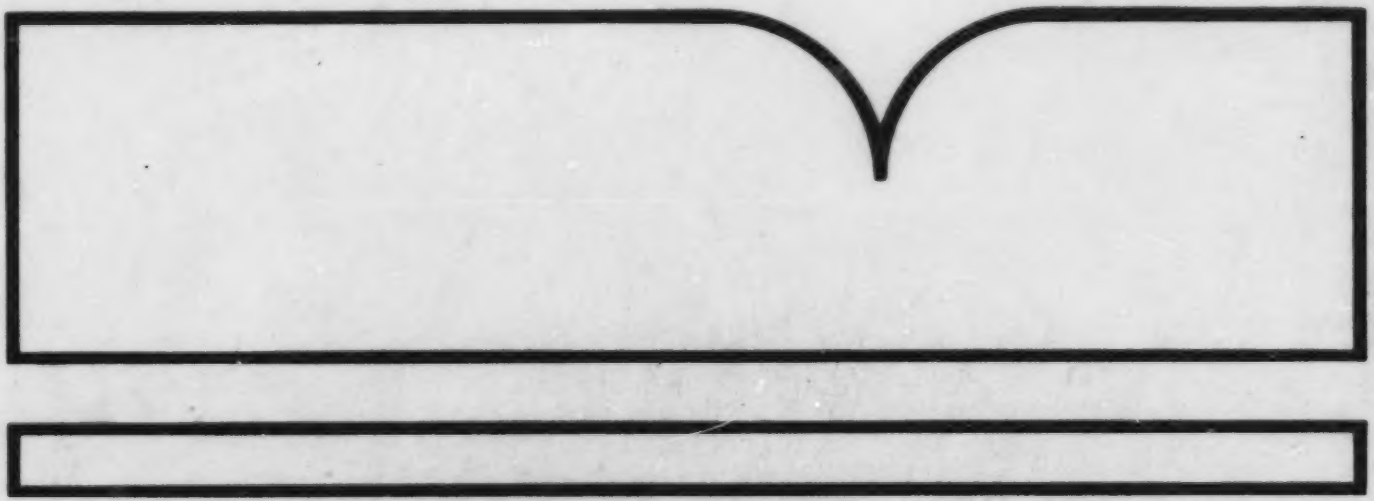

U.S. Department of Commerce
National Technical Information Service
NTIS

NOAA FORM 25-13 (2-73)

BIBLIOGRAPHIC DATA SHEET

U. S. DEPARTMENT OF COMMERCE
NATIONAL OCEANIC AND ATMOSPHERIC ADMINISTRATION

1. NOAA ACCESSION NUMBER	2.	3. RECIPIENT'S ACCESSION NUMBER
NOAA-81062609		PB81 234114

4. TITLE AND SUBTITLE

Environmental Effects of Pollutants from Coal Combustion:
2. The Colstrip, Montana, Power Plant

5. REPORT DATE

April 1981

6.

7. AUTHOR(S)

C.C. Van Valin, R.F. Pueschel, and D.L. Wellman

8. REPORT NO.

NOAA-TM-ERL OWRM-3

9. PERFORMING ORGANIZATION NAME AND ADDRESS

NOAA, Environmental Research Laboratories,
Boulder, CO, 80303
Office of Weather Research and Modification

10. PROJECT/TASK NO.

11. CONTRACT/GRANT NO.

Interagency Agreement
IAG79BEG/EHE-625/D5-E693

12. SPONSORING ORGANIZATION NAME AND ADDRESS

Same; and
U.S. Environmental Protection Agency

13. TYPE OF REPORT AND PERIOD COVERED

Tech. Memo.

14.

15. PUBLICATION REFERENCE

NOAA Technical Memorandum ERL OWRM-3, April 1981. 67 p, 25 fig, 9 tab, 33 ref.

16. ABSTRACT

Aerosol samples from the plume of the Colstrip, Montana, power plant were alanyzed for the presence of sulfates and nitrates with the transmission electron microscope using the $BaCl_2$ and Nitron tests. Plume profile measurements provided width and thickness dimensions that could be compared to the estimations obtained from numerical plume models. Tracking of the plume of the Colstrip power plant plume with the aircraft provided some examples of plume trajectories that were apparently influenced by the underlying terrain by being diverted by as much as 20° from the wind direction at plume altitute, or by being ducted along a valley. Ice nuclei measurements on plume samples, as done with the filter and the acoustic counter methods are in conflict, with the former method indicating no difference in ice nucleus concentrations between plume and ambient atmosphere, and the latter showing an increase of an order of magnitude, or more, in the plume. The difference in response between the two methods may be due to the deactivation of the deposition and condensation-followed-by-freezing modes of nucleation by the surface adsorption of soluble sulfates. (Author modified)

17. KEY WORDS AND DOCUMENT ANALYSIS

17A. DESCRIPTORS

*Coal, *Combustion, *Pollutants, *Aerosols, Sulfates, Nitrates, Plumes, Condensation nuclei

17B. IDENTIFIERS/OPEN-ENDED TERMS

Montana, Environmental effects, Ice nuclei, Colstrip power plant

17C. COSATI FIELD/GROUP

4B, 13B

18. AVAILABILITY STATEMENT

Released for distribution: Elaine S Dowse

19. SECURITY CLASS (This report)	21. NO. OF PAGES
UNCLASSIFIED	68 p.
20. SECURITY CLASS (This report)	**22. PRICE**
UNCLASSIFIED	

NOAA FORM 25-13 (2-73) SUPERSEDES ALL PREVIOUS EDITIONS.

☆ U.S. GPO:1976-0-665-661 1159

81062609

PB81-234114

NOAA Technical Memorandum ERL OWRM-3

ENVIRONMENTAL EFFECTS OF POLLUTANTS FROM COAL COMBUSTION:

2. THE COLSTRIP, MT POWER PLANT

C. C. Van Valin
R. F. Pueschel
D. L. Wellman

Office of Weather Research and Modification
Boulder, Colorado
April 1981

REPRODUCED BY
NATIONAL TECHNICAL
INFORMATION SERVICE
U.S. DEPARTMENT OF COMMERCE
SPRINGFIELD, VA 22161

noaa NATIONAL OCEANIC AND ATMOSPHERIC ADMINISTRATION / Environmental Research Laboratories

NOAA Technical Memorandum ERL OWRM-3

ENVIRONMENTAL EFFECTS OF POLLUTANTS FROM COAL COMBUSTION:

2. THE COLSTRIP, MT POWER PLANT

C. C. Van Valin
R. F. Pueschel
D. L. Wellman

Atmospheric Chemistry Program

Submitted to EPA in partial fulfillment of the requirements
of Interagency Agreement IAG79BEG/EHE-625/D5-E693

Office of Weather Research and Modification
Boulder, Colorado
April 1981

UNITED STATES DEPARTMENT OF COMMERCE
Malcolm Baldrige, Secretary

NATIONAL OCEANIC AND ATMOSPHERIC ADMINISTRATION
James P. Walsh, Acting Administrator

Environmental Research Laboratories
Joseph O. Fletcher, Acting Director

NOTICE

The Environmental Research Laboratories do not approve, recommend, or endorse any proprietary product or proprietary material mentioned in this publication. No reference shall be made to the Environmental Research Laboratories or to this publication furnished by the Environmental Research Laboratories in any advertising or sales promotion which would indicate or imply that the Environmental Research Laboratories approve, recommend, or endorse any proprietary product or proprietary material mentioned herein, or which has as its purpose an intent to cause directly or indirectly the advertised product to be used or purchased because of this Environmental Research Laboratories publication.

CONTENTS

		Page
ABSTRACT		v
1.	Introduction	1
2.	Secondary Particle Formation	5
3.	Particle Size Distributions	19
4.	Plume Dispersion	26
5.	Plume Trajectories	35
6.	Particle Composition	40
7.	Ice Nuclei	48
8.	Cloud Condensation Nuclei	54
9.	Plume Exposure - Hay Coulee	56
10.	Conclusions	58
11.	References	59

Environmental Effects of Pollutants from Coal Combustion:

2. The Colstrip, Mont., Power Plant

C. C. Van Valin, R. F. Pueschel, D. L. Wellman

ABSTRACT

Aerosol samples from the plume of the Colstrip, MT, power plant were analyzed for the presence of sulfates and nitrates with the transmission electron microscope using the $BaCl_2$ and Nitron tests. Almost all particles of $r < 0.3$ μm that were collected 8 km (5 mi) or more downwind from the plant were found to contain sulfate and many were exclusively sulfate, without a mineral nucleus. Many of the particles of $r > 1$ μm have an adsorbed layer of sulfate. There are few nitrate-containing particles of $r < 0.3$ μm; most nitrate-containing particles are found to have $r > 0.5$ μm. The explanation is that NO_2, formed from the oxidation of NO, is itself readily oxidized to HNO_3 by OH in the vapor phase or by H_2O in solution droplets. The HNO_3, or its mineral salt, is very hygroscopic and readily absorbs H_2O from the atmosphere, thus forming large particles. In plume samples collected ~ 1.6 km (1 mi) downwind and analyzed with the scanning electron microscope with energy dispersive X-ray analysis, two-thirds of the particles of $r > 0.1$ μm were spherical. Almost all of the spherical particles contained both Si and Ca, with about half containing S.

Particle flux measurements showed that the formation rate of particles in the plume is $\sim 10^{16}$ s^{-1}, with variation depending upon solar energy input and temperature, in addition to the emission rate of SO_2. This formation rate is satisfied with a conversion rate of SO_2 to sulfate of ~ 1 percent per hour. Most of the new volume formation shows up quickly in the accumulation mode, apparently through the mechanisms of gas deposition on existing aerosols, or by rapid growth of nuclei mode particles through coagulation. On the order of 90 percent of the new volume (at least regarding particles of $r < 0.25$ μm) is in the accumulation mode particles, modal radius about 0.06 μm. The modal radius increases with increasing reaction time, while the number of particles per unit volume decreases because of dilution and coagulation.

Plume profile measurements provided width (y) and thickness (z) dimensions that could be compared to the estimations obtained from numerical plume models. The predicted width was usually less than measured, whereas the predicted thickness was much larger than measured. The differences between predicted and measured vertical dimensions are partly the consequence of the strong dependence of vertical extent on atmospheric stability.

Tracking of the plume of the Colstrip power plant plume with the aircraft provided some examples of plume trajectories that were apparently influenced by the underlying terrain by being diverted by as much as 20° from the wind direction at plume altitude, or by being ducted along a valley.

Ice nuclei measurements on plume samples, as done with the filter and the acoustic counter methods are in conflict, with the former method indicating no difference in ice nucleus concentrations between plume and ambient atmosphere, and the latter showing an increase of an order of magnitude, or more, in the plume. The difference in response between the two methods may be due to the deactivation of the deposition and condensation-followed-by-freezing modes of nucleation by the surface adsorption of soluble sulfates.

The Hay Coulee field site was apparently exposed to the power plant plume for a total of about 30 h during 340 h of observation from 20 August to 3 September 1977. Plume exposures were characterized by wide variations of plume constituent concentrations, varying from near background to maximum values within minutes. For 21 different plume exposure periods, the maximum condensation nuclei concentrations were $12.2 \pm 9.8 \times 10^3$ cm $^{-3}$ (mean and 1 sigma standard deviation).

1. Introduction

In May 1975 the Atmospheric Chemistry Program (ACP) group of the Air Resources Laboratories, formerly of the Atmospheric Physics and Chemistry Laboratory, began a research project at the Hay Coulee field site, 12 km southeast of Colstrip, Montana. The purpose of the work was to characterize the aerosols found at the Hay Coulee location downwind from Colstrip prior to start-up of the plant and subsequently to determine the cloud and weather modification potential of the smoke plume. Study of the plume of the Montana Power Company coal-fired electric generating plant at Colstrip continued into 1979. During each of two field periods in 1975, 1976 and 1977 the ACP mobile laboratory was used at the Hay Coulee site; the specific intervals were:

Year	Spring	Fall
1975	18 May - 15 June	17 Aug - 15 Sept.
1976	21 May - 5 June	20 Aug. - 11 Sept.
1977	21 May - 4 June	20 Aug. - 4 Sept.

The ACP research aircraft was utilized during each of these field periods; in addition research flights were conducted in February 1977, June 1978, and February and March 1979. Three aircraft were used in succession, a 4-place, single-engined Cessna 182, a 6-place, single-engined Cessna 206, and a twin-engined Aero-Commander 680E. The Cessna 182, used during 1975, carried, at various times, a condensation nucleus counter, filter collectors, air and surface temperature sensors, a nephelometer, and an ozone analyzer. The Cessna 206 was used during 1976 and 1977; to the previous instruments were added a NO-NO_x analyzer, a cloud condensation nucleus counter, a sulfur dioxide analyzer and an 8-channel analog recorder. The AeroCommander 680E was

outfitted in May 1978 and has been used to date. Equipment carried aboard this aircraft is listed in Table 1; the notable additions are the Particle Measuring Systems, Inc. particle size measuring probes, the pulsed fluorescence sulfur dioxide analyzer to replace the Theta Sensors, Inc. instrument, the magnetic tape data acquisition system, and the electric field measuring instrument.

The Colstrip plant is a modern plant with advanced emissions controls and it has been regarded by the ACP group as an appropriate example with which to compare the Four Corners Powerplant which is less well controlled, regarding the effects of the emissions on the environment. The Colstrip powerplant has two pulverized-coal-burning units, each with a gross design output of 358 megawatts. Combustion effluents pass through alkaline fly ash-lime scrubbers, resulting in the SO_2 emission of approximately 285 g s^{-1} per unit at maximum load; the maximum particulate emission rate is ca. 46 g s^{-1}. Coal consumption at maximum load is rated at 98 kg s^{-1} assuming the use of coal with a heating value of 4.86×10^6 gram calories kg^{-1}. Unit 1 began operating in September 1975, with unit 2 start-up in July 1976.

Colstrip is located in southeastern Montana, in a region of forested buttes and steep-sided valleys, or coulees (Figure 1). The predominant agriculture is cattle ranching, as appropriate to the semi-aridity of the area, with some hay and dry-land wheat production. The two major ecosystems of the area are ponderosa pine-skunkbush and cool season-short grass (Gordon et al., 1978). The wind direction is predominantly west-northwest. The plant site elevation is 989 m (3245 ft.) and the smoke stacks are 152 m (500 ft.) tall. The closest terrain that exceeds the elevation of the stack tops is about 18 km (11 mi) west-southwest of the plant site on the east slope of the Little Wolf Mountains, where the maximum elevation is 1470 m (4820 ft.). To

TABLE 1. -- LIST OF INSTRUMENTS INSTALLED IN IN-SITU SENSING AIRCRAFT

PARAMETER	METHOD	INSTRUMENT MANUFACTURER/MODEL	TYPICAL OPERATING RANGE	MINIMUM DETECTABLE CONCENTRATION
Cloud Condensation Nuclei	Thermal Diffusion Chamber Photography	NOAA	200-2000 cm^{-3}	20 cm^{-3}
Aitken Nuclei	Expansion Chamber	Environment-one/RICH 100 Gardner/7000 4 G 2	300 to 10^7 cm^{-3}	1 x 10^2 cm^{-3}
Light Scattering Coefficient	Integrating Nephelometer	MRI 1550	0 - 10 x $10^{-4}m^{-1}$	.15 x $10^{-4}m^{-1}$
Temperature	Platinum Resistance	Rosemount 102 AN 1 AF	-40° to +40°C	
Relative Humidity	Thermoelectric Dew Point	GE 1011	-75°C to 50°C	
Ozone	Chemiluminescence	ML 8410	0 - 5 ppm	5.0 ppb
Nitric Oxide	Chemiluminescence	ML 8440	0 - 5 ppm	5.0 ppb
Nitrogen Dioxide	Chemiluminescence	ML 8440	0 - 5 ppm	5.0 ppb
Sulfur Dioxide	UV Pulsed Fluorescence	Teco 43	0 - 5 ppm	2.0 ppb
Aerosol Size	Aerosol Filtration Electron Microscopy	NOAA Sampler RCA TEM		5.0 cm^{-3}
Aerosol Composition	Aerosol Filtration Electron Microscopy X-ray Spectrometry	NOAA Sampler Coates & Welter SEM Kevex 5000		5.0 cm^{-3}
Ice Nuclei	Aerosol Filtration	Thermal Diffusion Chamber, NCAR		.5 cm^{-3}
Aerosol Size Distribution	He-Ne Laser Light Scattering	Particle Measuring Systems ASASP-X, FSSP	0.08-50 μm	
Potential Gradient	Electric Field Mill	NOAA	0-10^6 volts/meter	1 volt/meter
Infrared Radiation	Bead Thermistor	Barnes, PRT-5	-20 - +75 C	
Data Acquisition	Digital Processing	Particle Measuring Systems DAS 64		
	Magnetic Tape Recording	Pertec F6x9 Formatter Pertec T7640 Transport		
	Digital Printer	HP 5055A		
	Analog Recording	Gulton Tmd 840/S-1289		

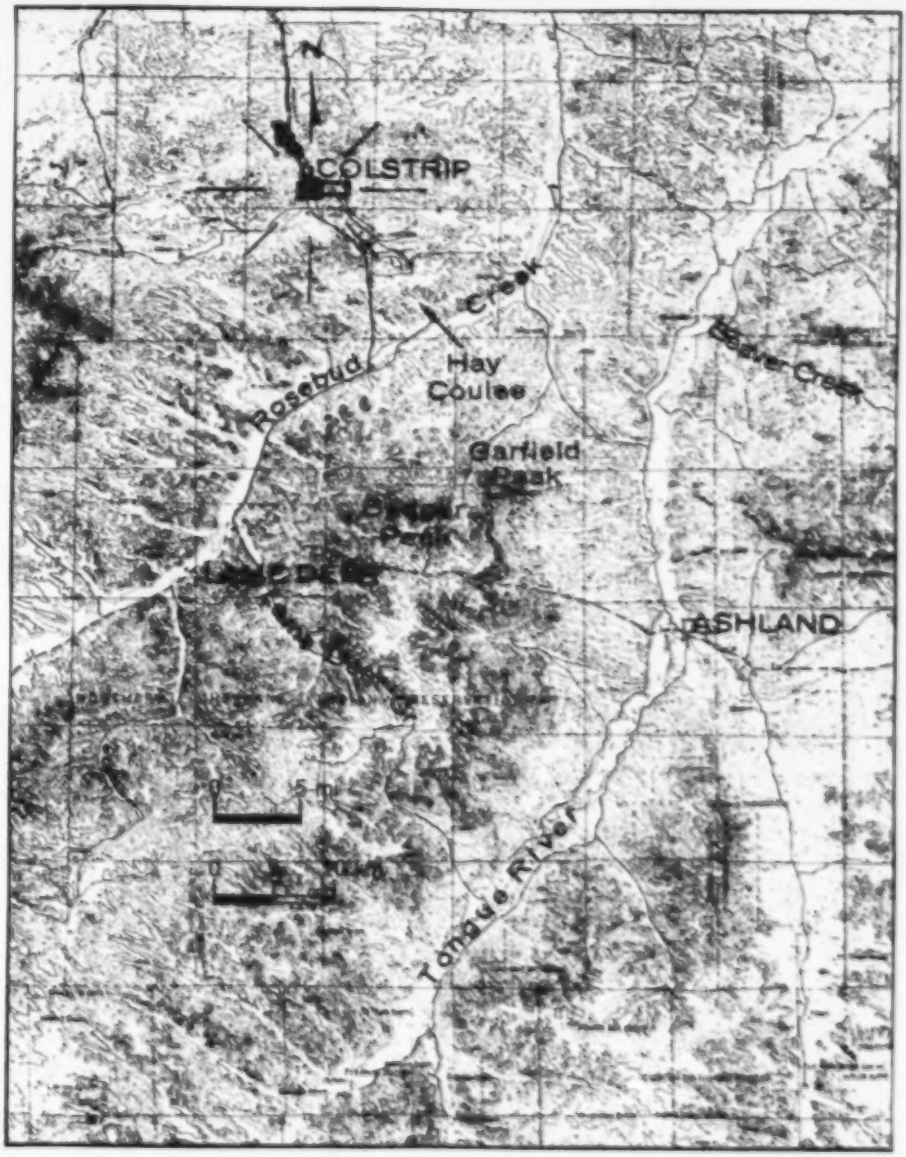

Figure 1. Topographic map of the Colstrip area. Contour intervals are 30.5 m (100 ft.). (U. S. Geological Survey, 1963)

the north the terrain gradually slopes down to the Yellowstone River Valley (45 km, 28 mi); east and south of the plant the terrain is lower than ca 1000 m (3300 ft.) as far as the slopes of Badger and Garfield Peaks to the south-southeast in the Northern Cheyenne Indian Reservation and of Cook Mountain to the southeast in the Custer National Forest, 24 and 41 km (15-25 mi), respectively.

The elevation at the mobile laboratory site at Hay Coulee is 930 m (3050 ft.), located on a four percent hillside sloping up to the south, west and north. The coulee bottom ~ 0.5 km east, drains south-southeast to Rosebud Creek. The upper, or northwest, end of the coulee is about 900 m (3250 ft.) at a distance of about 3 km. Upper elevations in the coulee support a sparse Ponderosa pine forest; the remainder of the range is dominated by western wheatgrass and big sagebrush in association with prairie junegrass and Japanese brome.

This summary is based largely on materials from which published papers have been derived. These include Abshire et al., 1978; Van Valin and Pueschel, 1978; Van Valin et al., 1979; Van Valin et al., 1980 a and b; Van Valin and Pueschel; to be published.

2. Secondary Particle formation

Due to the great efficiency with which primary (flyash) particle emissions are controlled, secondary aerosols are the particulate pollutants of greatest concern. Sulfur dioxide may be oxidized in solution in fog and cloud droplets in the presence of NH_3; the reaction is catalyzed by trace metal ions. The oxidation of SO_2 may also occur at the surfaces of particles, such as in the commercial production of sulfuric acid over platinum catalysts. A third category is most important in the oxidation of SO_2 in the atmosphere, viz., gas phase reactions, primarily, perhaps exclusively, involving

photochemical processes. These reactions are preceded by free radical generation during irradiation of NO-NO_2 and olefins in air. The formation of new particles in SO_2 polluted atmospheres follows gas phase oxidation. The free radical species, principally hydroxyl, OH, hydroperoxyl, HO_2, and peroxyalkyl, RO_2, operate through reactions such as:

$$SO_2 + OH + M \rightarrow HSO_3 + M \quad (1)$$

$$SO_2 + HO_2 \rightarrow SO_3 + OH \quad (2)$$

$$SO_2 + RO_2 \rightarrow SO_3 + RO \quad (3)$$

The HSO_3 and SO_3 are then rapidly converted to H_2SO_4 (Friedlander, 1978). Condensable molecules may form clusters of molecules or may deposit on existing particles. The original nuclei are believed to grow to diameters of 0.0075 μm in tens of seconds (Whitby, 1978) but for particles of diameter greater than 0.0075 μm the homogeneous coagulation rate is slower to a sufficient degree that the size distribution remains unimodal near 0.01 μm for a matter of hours (Clark and Whitby, 1975; Hidy and Lilly, 1965). However, the rate of heterogeneous coagulation of nuclei and accumulation mode particles is two to three times greater, thus providing a mechanism for the rapid transfer of mass to accumulation mode particles. These particles are sufficiently large to show environmental effects. The most important of these is probably the condensation of water on these particles, resulting in their growth to haze particles or cloud drops.

In addition, about 95 percent of new sulfate volume results from condensation, with only about 5 percent from homogeneous nucleation; the critical diameter for condensational growth is about 0.035 μm (Whitby, et al., 1978). This further emphasizes the existence of accumulation mode particles, of diameter 0.15 - 0.2 μm, as the long-lived species predominant in number concentration, and constituting the repository of mass from the gas-to-

particle process that is subject to long-distance transport (Pueschel and Mamane, 1979).

Samples of plume aerosol particles were collected on electron microscope screens mounted in front of the impactor jet nozzles of a four-stage Casella cascade impactor carried on the research aircraft. Diameters of particles collected were from 0.2 to 2.0 μm. The screens were vacuum coated with $BaCl_2$ for analysis of the sample for the presence of sulfate (Mamane and de Pena, 1978), or with nitron (1,4-diphenyl-3,5-endoanilino-4,5-dihydro-1, 2,4-triazole) for nitrate determination (Bigg et al., 1974; Mamane and Pueschel, 1980) with the transmission electron microscope (TEM).

Figure 2 shows photomicrographs of particles collected on a $BaCl_2$-coated grid that was mounted in the fourth (final) stage of the cascade impactor. The network of small, elongated particles of uniform size and distribution is the $BaCl_2$ substrate. The more or less circular spots of a larger size than the $BaCl_2$ are the reaction product from the $BaCl_2$ and the sulfate particles that impacted on the grid. When viewed in the TEM, only four (or 15 percent) of the darkest spots in the left-hand photomicrograph have opaque centers that are fly ash particles. The diameters of the $BaSO_4$ reaction spots are approximately twice those of the original sulfate particles; the smallest particles that appear in these photomicrographs were therefore about 0.2 μm initial diameter, corresponding to the cutoff diameter of the collection apparatus.

Figure 3 shows photomicrographs of particles collected on grids that were coated with nitron before (right) or after (left) collection of the sample. The nitron method is a specific test for nitrate by the formation of needle-like crystals or masses of needles. There are no nitrate-containing particles in the left-hand photomicrograph, and only two (or 9 percent) in the right

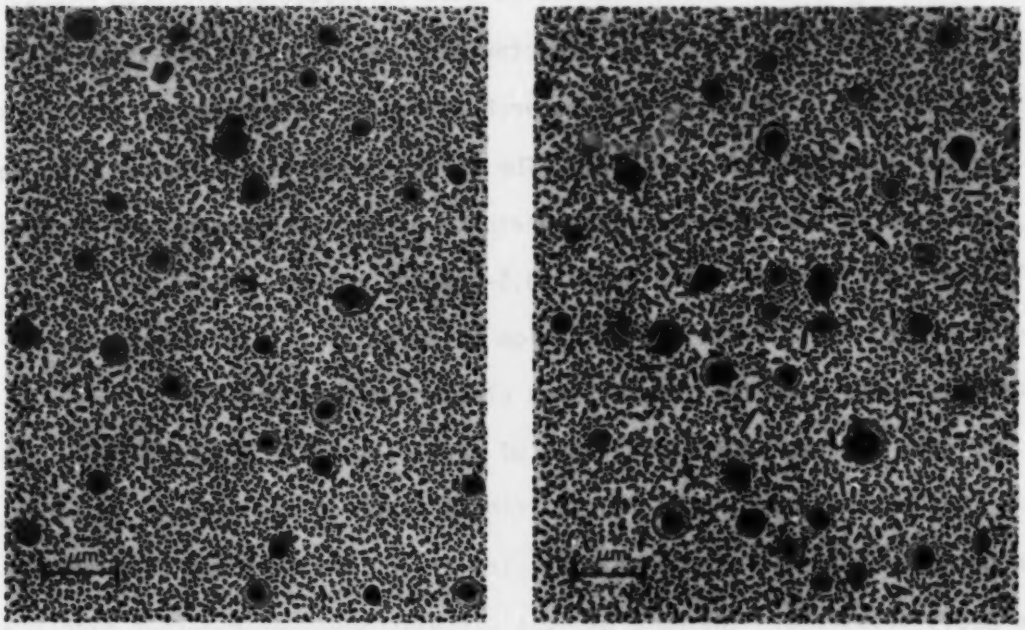

Figure 2. TEM photomicrographs of particles collected on the fourth stage of a Casella cascade impactor. Elongated particles of uniform dispersion are the $BaCl_2$ coating; round spots indicate sulfate particles that have reacted with the $BaCl_2$, and are about double the diameter of the original particle. The left photomicrograph includes several particles that include mineral (or fly ash) centers.

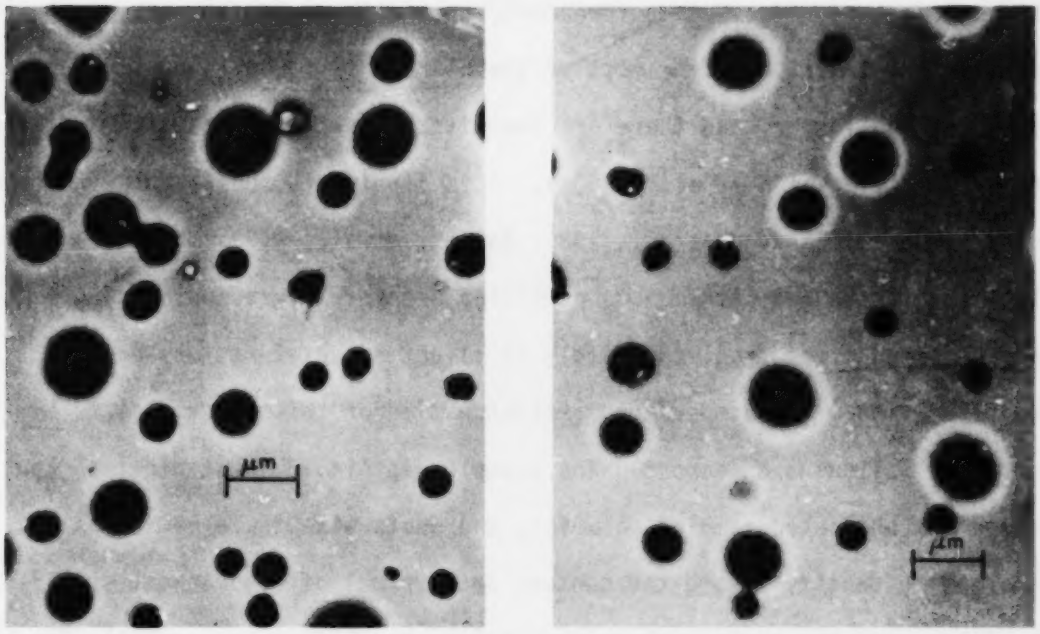

Figure 3. TEM photomicrographs. Left: particles collected on an impactor grid that was coated with nitron following collection. Right: grid was coated with nitron before sample collection. Spots with clear halos that shade into a darker center represent sulfates and are about three times the diameter of the particle they represent.

that may contain nitrate. Typically these impactor samples from power plant plumes do not show appreciable numbers of nitrate particles on the fourth stage impactor grids, but do frequently show nitrate in the next larger (third stage) size fraction, i.e., most of the nitrate is found in particles of 1 μm diameter and larger, and there are few nitrate-containing particles smaller than 1 μm (Van Valin et al., 1980a). This finding is consistent with those of other studies (Parungo et al., 1980; Barrett et al., 1979a). The explanation is that nitrate and nitric acid particles are very hygroscopic and grow to above-micron-sized droplets rapidly at slight supersaturations or even subsaturation. The atmospheric residence time of these particles is limited by rapid fallout and washout. The examples in Fig. 3 are typical of fourth-stage nitron-coated samples, however, the spots with the clear halos and increasing density toward the centers are typical of (though not specific for) sulfates, and the spots with neither halos nor shading are probably fly ash. Fly ash or other mineral particles with sulfate coatings would show as uniformly dense, sharp-edged spots surrounded by the clear halo (Mamane and Pueschel, 1979). In the left-hand photomicrograph there are two particles that may be mineral, with very faint halos; most of the rest are probably sulfates. The right-hand example includes eight spots that are probably fly ash particles of ~ 0.5 μm diameter without the sulfate coating. The diameters of the spots produced by sulfate on nitron are about three times those of the original particles; thus, the sulfate particles in these two nitron-coated samples were from 0.2 to 0.6 μm diameter, approximately. It is apparent in these examples that the smallest particles collected on the electron microscope screen were composed of sulfate without a mineral nucleus. It can reasonably be assumed that the same would be true of particles of sizes smaller than the impactor cutoff diameter. We conclude, therefore, that

sulfates dominate in the small-size region of the plume particle size spectrum.

Measurements done on 29 August 1977 in the plume at two distances downwind from the power plant provided an opportunity for further assessment of the fate of the nitrogen compounds. At this time repeated penetrations were made through the densest part of the plume; the data collected are presented in Table 2. Because of a malfunction in the nitrogen oxides analyzer, the NO_2 could not be accurately measured during the rapidly changing concentrations encountered during the 5 km downwind plume penetrations; no more can be said of the NO_2 concentration at the densest part of the plume than that it was less than 40 ppb but greater than 0.

The decrease in NO_x ($NO + NO_2$) concentration from the shorter to the longer distance, equivalent to dilution by a factor of 5-6 on the average, is greater than would be expected from simple plume dilution. The total particle concentration (AN), which is reduced by a factor of about 3.8, probably gives a better picture of plume dilution. To use the AN concentrations in this way requires the assumption that particle loss through coagulation and settling, and particle gain through gas-to-particle generation processes, are small with respect to the measured concentrations at this time of the morning and over the limited time of plume travel between these two measurement locations. If reduced by a factor of 3.8 the NO concentration would be about 78 ppb, or ~ 28 ppb higher than the actual measured value. The NO is subject to reaction with O_3, which is brought into the plume by mixing and diffusion:

$$NO + O_3 \rightarrow NO_2 + O_2 \,. \qquad (4)$$

The 28 ppb of NO would be equivalent to 43 ppb (mass) of NO_2, leaving ~ 29 ppb of NO_2 (43 ppb possible, minus 14 ppb measured) unaccounted for, in addition to the NO_2 present in the plume at 5 km downwind. The probable sink for the

Table 2.--Concentrations of trace constituents (means and standard deviations) during repeated aircraft penetrations of the Colstrip powerplant plume on 29 August 1977

Location	Time (MDT)	NO (ppb)	NO_2 (ppb)	b_{scat} (x 10^{-4} m^{-1})	O_3(ppb)	AN (x 10^3 cm^{-3})
5 km downwind Max at 1310 m MSL	0738-0755	300 ± 110 (n = 15)	< 40	1.31 ± 0.32 (n = 15)	0	17 ± 5 (n = 13)
Background	0738-0755	~ 5	< 5	0.21 ± 0.05 (n = 29)	66 ± 2 (n = 23)	~ 1
16 km downwind Max at 1220 m MSL	0800-0818	50 ± 20 (n = 10)	14 ± 5 (n = 9)	0.50 ± 0.08 (n = 12)	15 ± 6 (n = 11)	5 ± 4 (n = 10)
Background	0800-0818	~ 5	< 5	0.20	67 ± 2 (n = 25)	~ 1

n = the number of data points

NO_2 has been indicated in work reported by Parungo et al. (1980) and Van Valin et al. (1980a) on the formation of nitrate particles in polluted atmospheres. The proposed mechanism is that NO_2, being hygroscopic, absorbs and dissolves in water to form nitric acid solution droplets predominantly in the size range 1-2 μm diameter. The relative humidity was about 95 percent at the Hay Coulee field site until surface heating began following sunrise, but then dropped sharply; r.h. was about 85 percent at 0730 MDT and about 65 percent at 0800 MDT. Similar conditions are assumed at the flight altitude of 275 m (900 ft.) AGL.

The O_3 concentration in the densest part of the plume is much less than would be calculated from simple dilution. The measured concentrations at 5 and 16 km downwind are 0 and 15 ppb, respectively. With the O_3 concentration in ambient air of 67 ppb, simple dilution would result in 50 ppb in the plume at 16 km. Taking into account the uncertainty in these measurements, the indicated deficit of 35 ppb of O_3 is roughly equivalent to the amount required to react with the deficit NO.

The preceding discussion is based on measured concentrations in the densest part of the plume. In order to assess change across the plume, NO, NO_2, and O_3 concentrations from locations representing various plume densities were plotted as NO_2 or O_3 vs. NO (Fig. 4). The two lines were obtained by a least squares fit; the coefficients of determination, r, were 0.76 and 0.81. (The background O_3 concentration of 67 ppb and NO and NO_2 of near zero, were not included in the curve fitting calculations.) Both NO_2 and O_3 are higher in the less dense portions, representing both more dilution and a greater degree of reaction between O_3 and NO, but the O_3 decline is in excess of that required to produce the small amount of NO_2 actually measured. Nitrate particle formation is the apparent sink for the unaccounted NO_2.

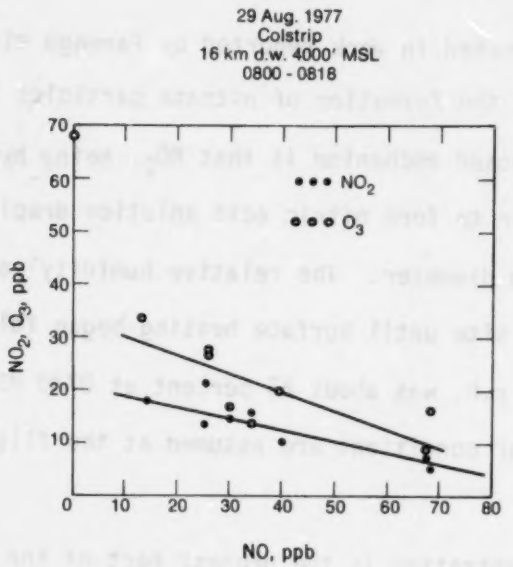

Figure 4. Least squares fit of NO_2 vs. NO and O_3 vs. NO in the Colstrip plume in regions of different plume densities. The coefficients of determination, r, were 0.76 and 0.81, respectively.

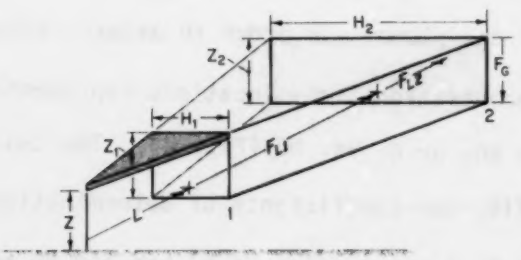

Figure 5. Schematic of the plume model employed in the particle flux calculations.

The presence of NO, NO_2 and O_3 in the atmosphere comprises a photochemical system during the day. Reaction (4) is very fast and proceeds almost to completion in the dark. During the day NO_2 is photolyzed by absorption of ultraviolet radiation

$$NO_2 \xrightarrow{h\nu} NO + O \qquad (5)$$

and leads to the formation of O_3

$$O + O_2 (+M) \rightarrow O_3 (+M) \qquad (6)$$

Reaction (6) is very fast; reaction (5) is the rate determining step. Under equilibrium conditions $d[O_3]/dt = 0$, and

$$\frac{[O_3][NO]}{[NO_2]} = \frac{k_2}{k_1} ,$$

theoretically a constant. In reporting measurements of the Labadie powerplant plume, White (1977) showed that $[O_3][NO]/[NO_2]$ achieved a rather noisy constant across the plume and in the surrounding atmosphere of roughly 10 - 50 ppb during the early afternoon. Calvert (1976) reported similar values in the Los Angeles basin during midday, but found very much higher values in the morning when the sun elevation angle was less than 30° and the atmospheric optical thickness to solar radiation was greater than 1.9 atmospheres. The model used by Calvert in this case predicts lower values early and late in the day for an equilibrated system. It appears that the high values actually found are indicative of a dynamic system undergoing introduction of a large amount of NO and which is far from photochemical equilibrium. The measurements shown in Fig. 4 were obtained with solar elevation angles of 15.9 to 19.1° and air masses of 3.1 to 2.6 atmospheres. The ratio $[O_3][NO]/[NO_2]$ was found to vary from about 160 ppb in the most

dense parts of the plume to about 14 ppb in the more dilute parts. Because of the low solar energy input (about 0.4 cal cm^{-2} min^{-1} at the Hay Coulee field site near the location and at the time of the plume measurements, compared to about 1.2 cal cm^{-2} min^{-1} maximum at midday as measured with a hemispheric pyranometer under quartz), gradual dilution of the plume, and apparent removal of NO_2 by absorption in water during the period of high humidity, the system is evolving principally through reaction (4).

Measurements of gas and particle concentrations both in and out of the Colstrip powerplant plume, and of the plume width and depth were accomplished with the aircraft and permitted the calculation of particle formation rates. From the AN measurements, we calculated particle fluxes through vertical plume cross-sections at various distances downwind from the powerplant. The fluxes were calculated by first integrating measured particle concentrations, corrected for background, over the respective plume cross-sections. The results were then multiplied by the average wind velocity $\bar{u}$ in the x direction. Figure 5 shows the box model that was adopted to calculate the fluxes. The net particle formation rate, $\frac{\Delta AN}{\Delta t}$, is the transport out of the box minus the transport into the box,

$$\frac{\Delta AN}{\Delta t} = F_{L_2} + F_G - F_{L_1},$$

where F_{L_2} is the flux through the vertical plume cross-section at distance L_2, F_{L_1} is the flux through a plume cross-section at distance L_1, and F_G is the vertical deposition flux between distances L_2 and L_1. Table 3 shows the results for three cases studied on February 16, August 31 and September 1, 1977. The net rate of increase in the particle population within the indicated 24.5 to 33 km long segment of the plume is found to be between 10^{15} and 10^{16} s^{-1}.

In the three examples of Table 3 the plume cross-sectional dimensions

Table 3.--Colstrip powerplant plume measured cross sectional area and calculated Aitken nucleus flux and particle production rates

	16 February 77	31 August 77	1 September 77
Downwind Distance (km)			
first	0.5	12	12
second	25	43	45
Plume Width (km)			
first	0.1	6	5.1
second	2.8	12	7.4
Wind Velocity ($m\ s^{-1}$)	6	8	6
Cross Sectional Area (cm^2)			
first	3.1×10^7	2.8×10^{10}	1.4×10^{10}
second	5.3×10^9	5.6×10^{10}	2.0×10^{10}
AN Flux (s^{-1})			
first	3.0×10^{14}	$4. \times 10^{16}$	2.3×10^{16}
second	4.1×10^{15}	5.1×10^{16}	3.4×10^{16}
Net Production (s^{-1}) (disregarding losses)	3.8×10^{15}	1.1×10^{16}	1.1×10^{16}

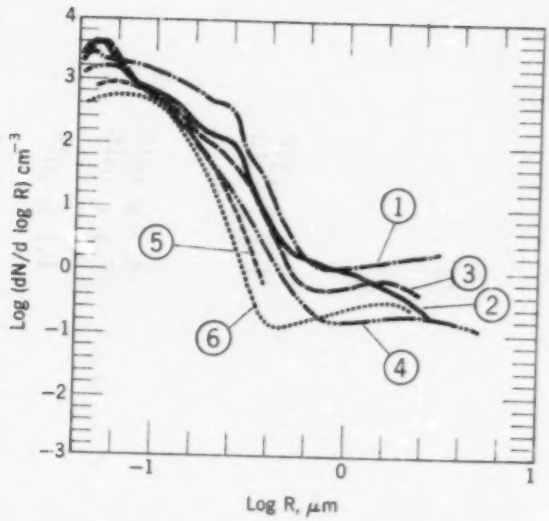

Figure 6. Aerosol size distributions measured in the plume of the Colstrip power plant, plus a background sample, 3 June 1978. The times (MDT, hr:min:sec) and locations are: (1) 6:15:34-6:15:44, less than 1 km d.w.; (2) 6:18:19 - 6:18:34, 10 km d.w.; (3) 6:29:29 - 6:30:04, 16 km d.w.; (4) 6:44:34 - 6:45:09, 48 km d.w.; (5) 6:51:49 - 6:52:09, 63 km d.w.; (6) 6:58:59 - 7:03:59, background, 65 km d.w.

were obtained by cross-wind flights through the plume at 100 ft (30 m) vertical intervals. The edge of the plume was judged to exist at the point where the AN concentration was about twice the noise level of the background measurements, i.e., when the concentration measured was different from local background by a few hunderd AN cm^{-3}. In the case of 16 Feb 77 the net particle production rate of 3.8×10^{15} s^{-1} is the difference between the measured particle flux 25 km downwind and the estimated flux 0.5 km from the plant. The 0.5 km estimate is based on the measured maximum concentration during a pass over the stacks and downwind in the plume. We assume this maximum concentration applies to the entire cross-section area, derived according to Turner (1970). It is probably not realistic to apply the maximum concentration to the entire area; on the other hand, the actual cross-sectional area may be somewhat larger than the theoretical prediction (Van Valin and Pueschel, 1981) and the particle flux, as estimated is probably realistic. In spite of the uncertainty of this estimate it is certain that the 0.5 km particle flux is small in comparison to the 25 km flux, i.e., the 25 km flux is composed almost entirely of secondary particles (in agreement with the conclusion of Hobbs et al., 1980).

3. Particle Size Distributions

Measurements of the size distributions of particles in the Colstrip plume and of background aerosols in the near vicinity were made during June 1978, Feb. 1979, and Mar 1979, with the Particle Measuring Systems, Inc., active scattering (ASASP-X) and forward scattering (FSSP) probes. In combination, these probes cover the radius interval from 0.05 μm to 23.5 μm in eight ranges of 15 bins each. Figure 6 shows the gamma distribution-fitted plots (Barrett et al., 1979) of numbers of particles per log radius interval versus the particle radius, in logarithmic scale, from plume and background measurements

on 3 June 1978. In Table 4 are listed the mean particle concentrations ($\overline{CN}$) during the indicated sampling periods as measured with the Environment/one condensation nucleus counter, the integrated number concentrations (N) in the size range covered by the plots of Figure 6, the mean Aitken nucleus ($\overline{AN}$) concentrations, here defined as $r < 0.047$ μm, obtained as the difference between $\overline{CN}$ and N, and the ordinate maxima of the fitted curves of Figure 6.

At the shortest distance from the power plant smoke stacks, i.e., < 1.6 km, the particle populations of all intervals across the size spectrum were greater than those found at greater distances, except in the interval from the 0.047 μm cutoff to about 0.07 μm. During the time of plume transport from a downwind distance of < 1.6 km to ~ 16 km, about 1.5 hr, the $r < 0.047$ μm particle fraction concentration was depleted to about one-third of the earlier concentration, the fraction of $0.047 < r < 0.07$ μm increased by one-third, and all fractions of $r > 0.07$ μm decreased markedly. A particle fraction of modal radius $r = 0.25$ μm appears in the measurements done at downwind distances of < 1.6, 10 and 16 km. This is probably a primary emittant; in view of the particle size it can be regarded as a conservative constituent of the plume, neither being augmented by secondary particle formation and growth nor depleted by removal by deposition or growth to larger sizes (McMahon and Denison, 1979; Whitby et al., 1978; Van Valin and Pueschel, 1981). The modal ordinate concentrations of the 0.25 μm mode as measured (Figure 6), and the concentration ratios thus derived can be used as indicators of plume dilution in the intervening distances. Accordingly, we estimate that the plume cross-sectional area had increased by a factor of 3.4 from the < 1.6 km to the 10 km location and by an additional factor of 2.3 at 16 km (7.8 x increase overall). In consequence the integrated particle

Table 4.--Statistics from the plume penetration flight of 3 June 1978, Colstrip, MT

Sample period, MDT, hr:min:sec	Location, km downwind	$\overline{CN}^{(1)}$ cm^{-3} ($x10^3$)	$N^{(2)}$ cm^{-3} ($x10^3$)	ordinate $max^{(3)}$ cm^{-3} ($x10^3$)	$\overline{AN}^{(4)}$ cm^{-3} ($x10^3$)	b_{scat} ($x10^{-4} m^{-1}$)
6:15:34-6:15:44	<1.6	23	1.4	2.9	22	1.75
6:18:19-6:18:34	10	11	1.2	4.0	10	0.85
6:29:29-6:30:04	16	8	1.1	4.0	7	0.75
6:44:34-6:45:09	48	2	0.7	1.7	1	0.45
6:51:49-6:52:09	63	<1	0.4	0.9	<1	0.38
6:58:59-7:03:59	65 (Background)	<1	0.3	0.6	<1	0.35

(1) $\overline{CN}$ = mean CN concentration during the sampling interval.

(2) N = integrated particle concentration, $r > 0.047$ μm, derived from the size distribution plots. Figure 6.

(3) maximum interval value, $r > 0.047$ μm, recorded on the size distribution plots, Figure 6.

(4) $\overline{AN}$ = mean AN concentration; the difference between $\overline{CN}$ and N.

concentration, N, of the gamma distribution curve (Table 4 and Figure 6) represents an increase by a factor of more than 6, and the one-third increase in the ordinate maximum, which occurred in the range $0.047 < r < 0.07$ μm, shows that close to an order of magnitude increase took place in this range. If one assumes a plume cross-sectional area of 2×10^{10} cm^2 at 16 km downwind, i.e., similar to that measured on 31 Aug. and 1 Sept. 1977, 12 km downwind from the plant (Table 3), the particle flux ($r > 0.047$ μm) at that point, with a wind velocity of 3 ms^{-1}, would be ca. 6.6×10^{15} s^{-1}. The flux of particles of this size range at < 1.6 km, with an estimated cross-sectional area of 2.6×10^9 cm^2, is calculated as 1.1×10^{15} particles s^{-1} (Table 5). The net increase in the concentration of particles of $r > 0.047$ μm in the intervening distance is then the difference between the two fluxes, or 5.5×10^{15} s^{-1}. In like manner the net particle concentration increase ($r > 0.047$ μm) between < 1.6 and 10 km is found to be ~ 2×10^{15} s^{-1}.

The AN ($r < 0.047$ μm) flux can also be estimated; the fluxes at < 1.6, 10 and 16 km downwind are then approximately 1.7, 2.6 and 4.2×10^{16} particles s^{-1} (Table 5). In considering this increase in AN with increasing distance (i.e., plume transport time) we must note a condition of uncertainty regarding the CN measurements at < 1.6 km downwind, viz., the CN counter output during the 10 s sampling period was offscale on the high side because of an inappropriate range setting. Within 10 s after this sample period, the range was changed to properly accommodate the greatest expected fluctuations; within another 5 s a plume parcel density peak was recorded on all instruments, including the nephelometer, which has a sample purging and output lag time about the same as the CN counter. The proportionality measured between the mean b_{scat} value from 6:15:34-6:15:44 MDT and the subsequent maximum recorded at 6:15:59 was applied to the CN measurement at 6:15:59 to arrive at the value

Table 5.--Particle flux estimations at 3 locations downwind from the Colstrip, MT, powerplant on 3 June 1978

Sample period MDT, hr:min:sec	location, km downwind	plume cross-sectional area assumed, cm^2 ($x10^{10}$)	AN flux s^{-1}($x10^{16}$)	AN mass flux, gs^{-1}(d=1.65 g cm^{-3}) nmr* = 0.005 mmr* = 0.0066	AN mass flux, gs^{-1}(d=1.65 g cm^{-3}) nmr = 0.01 mmr = 0.014	Particle flux s^{-1}($x10^{15}$) r>0.047 µm	Particle flux s^{-1}($x10^{15}$) 0.047<r <0.07 µm	mmr, µm (0.047 < r < 0.07 µm)	Particulate mass flux, gs^{-1}(d=1.65 g cm^{-3}) (0.047 < r < 0.07 µm)
6:15:34-6:15:44	<1.6	0.26	1.7	0.04	0.3	1.1	0.3	0.053	0.3
6:18:19-6:18:34	10	0.87	2.6	0.06	0.5	3.1	1.3	0.059	1.8
6:29:29-6:30:04	16	2.0	4.2	0.09	0.8	6.6	2.7	0.059	3.8

*nmr = number modal radius
mmr = mass modal radius

of 23 x 10^3 particles cm^{-3}. Thus, while this number, and the numbers derived from it, are regarded as realistic estimates, the uncertainty is greater than in the other plume samples.

As noted above, the AN population more than doubled between 1.6 and 16 km; this occurred while particles were being removed from the AN group ($r < 0.047$ μm) by particle growth through gas absorption and particle coagulation resulting in the beneficiation of the accumulation mode, $0.047 < r < 0.07$ μm, where the total net number increased by an order of magnitude. The measured mass modal radius (mmr) of the accumulation mode 16 km downwind was 0.059 μm, with a mass concentration of 0.63 ug m^{-3} (assume d = 1.65) indicating a mass flux of 3.8 g s^{-1}, compared with a mass flux of ~ 0.3 g s^{-1} in this size range at < 1.6 km downwind (Table 5). The size distributions of particles of $r < 0.047$ μm were not measured, so calculation of AN mass flux must depend upon size estimates, with the consequence that a wide band of mass flux must be postulated instead of a more specific value. Whitby et al. (1978) found the geometric number mean radius of the nuclei mode in the Labadie (St. Louis, MO) power plant plume to be 0.005 μm. Using this value as the number modal radius (nmr), and with a number distribution similar to that used by Whitby et al., we found a mmr of 0.0066 μm and a mass flux of ca. 0.09 g s^{-1} at a distance of 16 km (Table 5). Another plausible case with a nmr of 0.01 μm and a broader modal distribution produced, with the gamma distribution fit, a mmr of 0.014 μm and a mass flux of 0.8 g s^{-1}. The hypothetical curves upon which these numbers are based are shown in Figures 7 and 8. In the case with the smaller nmr the mass flux in the nuclei mode (AN) is insignificant and in the other example is ca. 20 percent of that from all particles of $r < 0.07$ μm. The net particulate mass increase with increasing distance downwind in both categories of $r < 0.07$ μm, as shown in Table 5

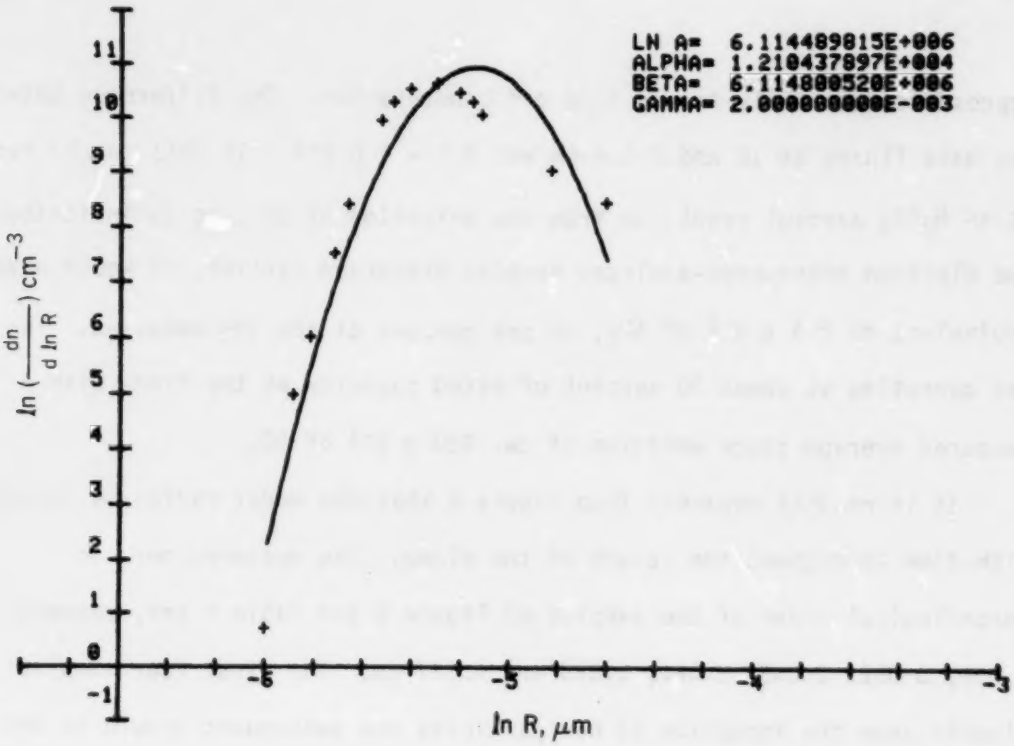

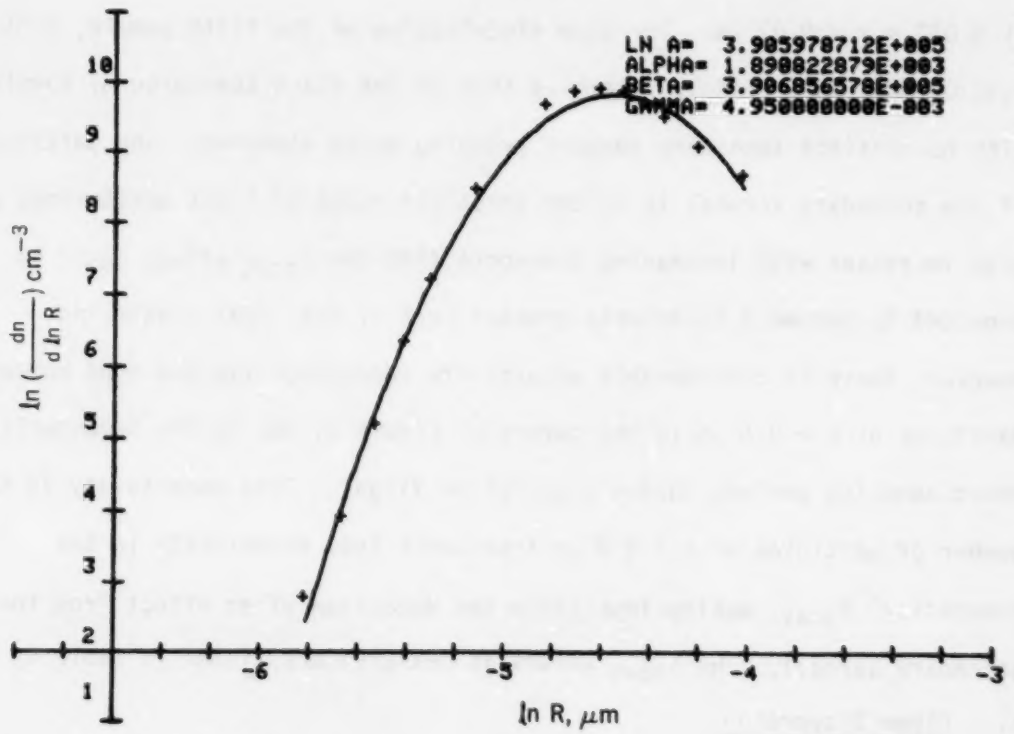

Figure 7. (Top) Gamma distribution fit (Barrett et al., 1979) of a hypothetical size distribution curve of nmr = 0.005 μm.

Figure 8. (Bottom) Same as Figure 7, nmr = 0.01 μm.

represents mass newly formed from gas condensation. The difference between the mass fluxes at 16 and < 1.6 km was 3.5 - 4 g s^{-1}. If this can be regarded as an H_2SO_4 aerosol resulting from the oxidation of SO_2, as is indicated in the electron microscope-analyzed samples discussed earlier, it would have been equivalent to 2-3 g s^{-1} of SO_2, or one percent of the SO_2 emission. The plant was operating at about 70 percent of rated capacity at the time, with a measured average stack emission of ca. 250 g s^{-1} of SO_2.

It is readily apparent from Figure 6 that the modal radius is increasing with time throughout the length of the plume. The measured nmr, in chronological order of the samples of Figure 6 and Table 4 are, respectively, 0.051, 0.052, 0.055, 0.061, 0.065 and 0.067 μm. The first four samples clearly show the formation of new particles and subsequent growth in the range of $0.047 < r < 0.07$ μm. The size distribution of the fifth sample, 6:51:49-6:52:09 MDT, more closely resembles that of the sixth (background) sample, with no distinct secondary aerosol grouping being apparent. The particle size of the secondary aerosol is in the threshold range of light scattering; as the size increases with increasing transport time the b_{scat} effect could be expected to become a relatively greater part of the total scattering. However, there is considerable uncertainty connected with the true numbers of particles of $r > 0.5$ μm in the curves of Figure 6, due to the necessarily short sampling periods during cross-plume flight. This uncertainty in the number of particles of $r > 0.5$ μm translates into uncertainty in the theoretical b_{scat}, making impossible the detection of an effect from the secondary aerosol. The b_{scat} values as measured are listed in Table 4.

4. Plume Dispersion

We present here several examples of plume profiles. Figures 9 and 10 show the Aitken Nuclei (AN) concentrations found in vertical and horizontal

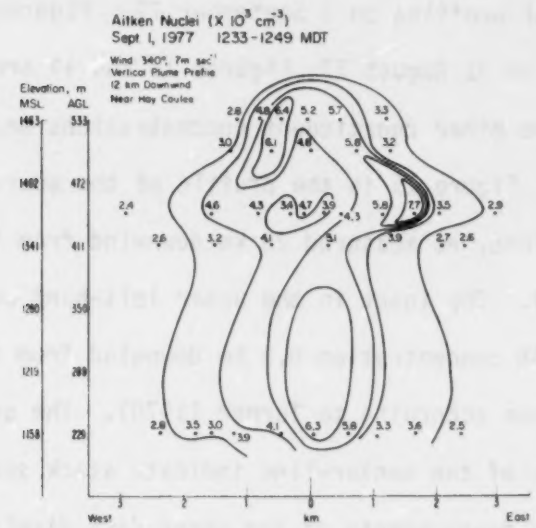

Figure 9. Vertical profile of the Colstrip power plant plume on 1 September 77, 1233-1249 MDT. The plume was not detected at 1524 m (5000 ft) MSL.

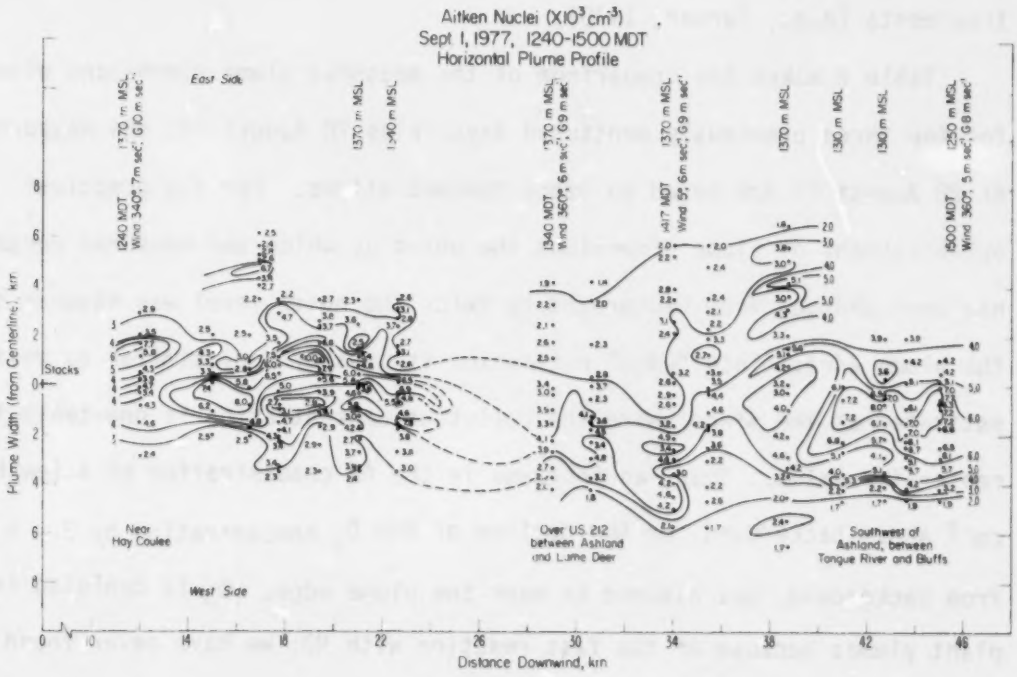
Aitken Nuclei (X10³ cm⁻³)
Sept 1, 1977, 1240-1500 MDT
Horizontal Plume Profile
East Side
West Side
Stacks
Plume Width (from Centerline), km
Distance Downwind, km
Near Hay Coulee
Over U.S. 212 between Ashland and Lame Deer
Southwest of Ashland, between Tongue River and Bluffs

Figure 10. Horizontal profile of the Colstrip power plant plume from 12 to 45 km downwind on 1 Sept. 77, 1240-1500 MDT. Plume traverses were conducted at the distances and altitudes as indicated.

cross-sectional profiles on 1 September 77. Figures 11 and 12 are similar profiles done on 31 August 77; Figures 13 and 14 are vertical and horizontal profiles of the other constituent concentrations measured at the densest part of the plume. Figure 15 is the profile of the powerplant plume representing AN concentrations, as measured 25 km downwind from the powerplant on 16 February 77. The inset in the upper left-hand corner of Figure 15 shows the measured AN concentration 0.5 km downwind from the stacks, and theoretical plume dimensions according to Turner (1970). The symbols on the x-axis 10 m on either side of the center-line indicate stack spacing and diameter.

The plume measurements on the three days display the inhomogeneities along the x, y, and z axes that are typical for single source plumes at a given instant. The inhomogeneity contrasts with the Gaussian distributions of plume properties along both the y and z axes that are predicted by theoretical treatments (e.g., Turner, 1970).

Table 6 makes the comparison of the measured plume dimensions with theory for the three previously mentioned days, plus 28 August 77; the measurements of 28 August 77 are based on ozone concentrations. For the practical establishment of plume dimensions the point at which the measured parameter had been changed from background by twice the noise level was assumed to mark the plume edge. This "edge" estimation is usually very similar to that estimated as the place where the pollutant concentration is one-tenth the centerline value. Thus, an increase in the AN concentration of a few hundred cm^{-3} above background, or the decline of the O_3 concentration by 3 - 4 ppb from background, was assumed to mark the plume edge. O_3 is depleted in power plant plumes because of the fast reaction with NO; we have never found an instance of O_3 augmentation in the Colstrip plume. O_3 depletion and AN augmentation are regarded by us as equally significant plume indicators. It

Table 6.--Measured and predicted dimensions for the Colstrip, Montana powerplant plume. The predicted dimensions are from Turner (1970); the indicated Pasquill stability classes were assumed on the basis of criteria regarding wind velocity, solar energy and cloud cover (Turner, 1970).

Downwind Distance (km)	Width (m)			Thickness (m)		
	Measured	Predicted		Measured	Predicted	
16 Feb 77		Stability Index D	C		Stability Index D	C
1/2	--	100		--	40	
8	>1800		1400	140-350		800
25	2800	2400		250	460	
28 Aug 77		Stability Index D	C		Stability Index D	C
4	900	500	740	440	160	440
12	1600 (max.) 1150 (ave.)	1300	2000	260	300	1200
31 Aug 77		Stability Index C	B		Stability Index C	B
12	5000	2000	2800	650	1200	3200
34	10500	4800	6800			
1 Sep 77		Stability Index D	C		Stability Index D	C
12	5500	1300	2000	330-550	300	1200
34	11500	3200	4800			

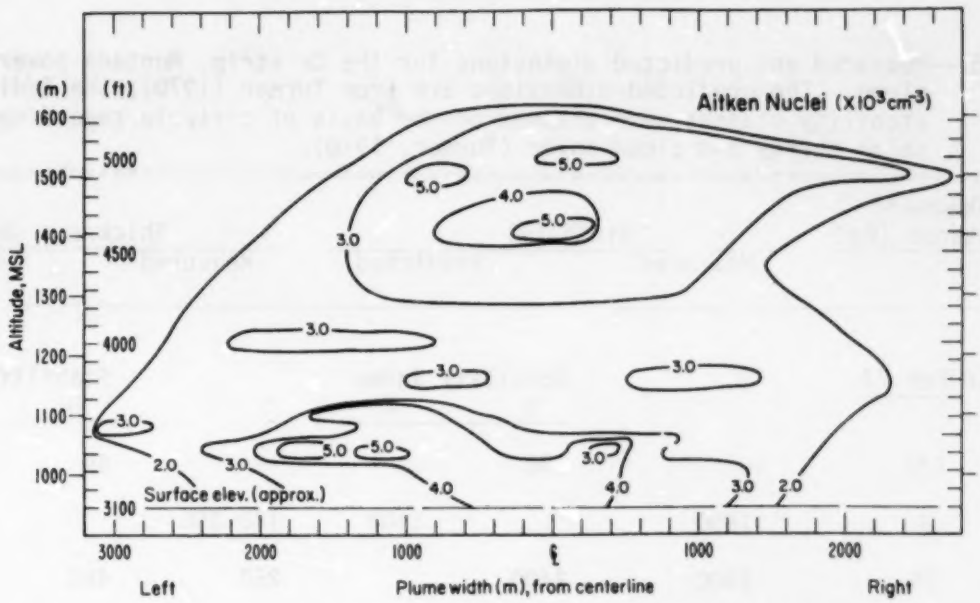

Figure 11. Vertical profile of the Colstrip plume on 31 August 77, 0915-1024 MDT. Plume traverses for this profile were done at 30 m (100 ft) intervals in descending order from 1615 m (5300 ft) MSL, where the plume was not detected, to 1006 m (3300 ft) MSL, which was the lowest safe flying altitude.

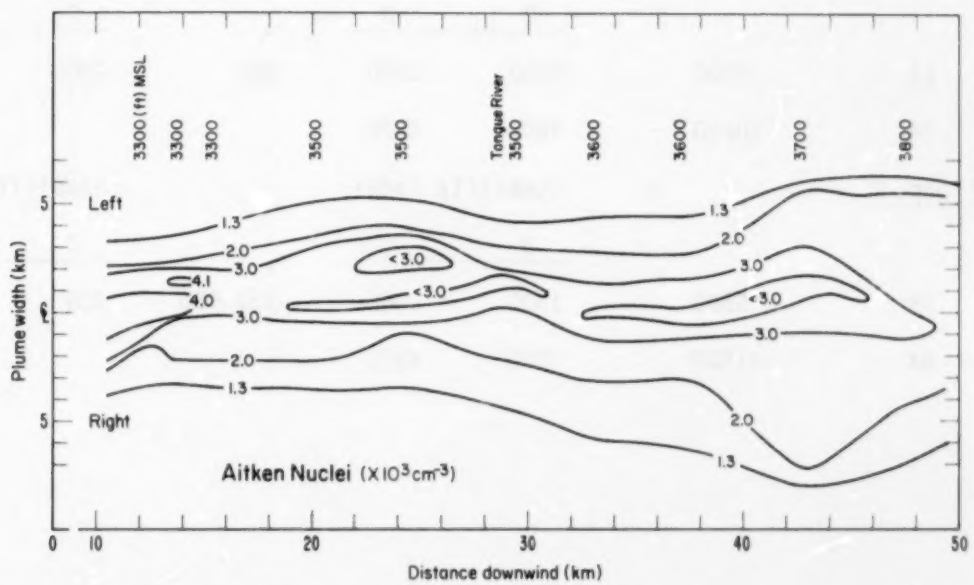

Figure 12. Horizontal profile of the Colstrip plume on 31 August 77, 1024-1140 MDT, constructed from the data of 10 traverses.

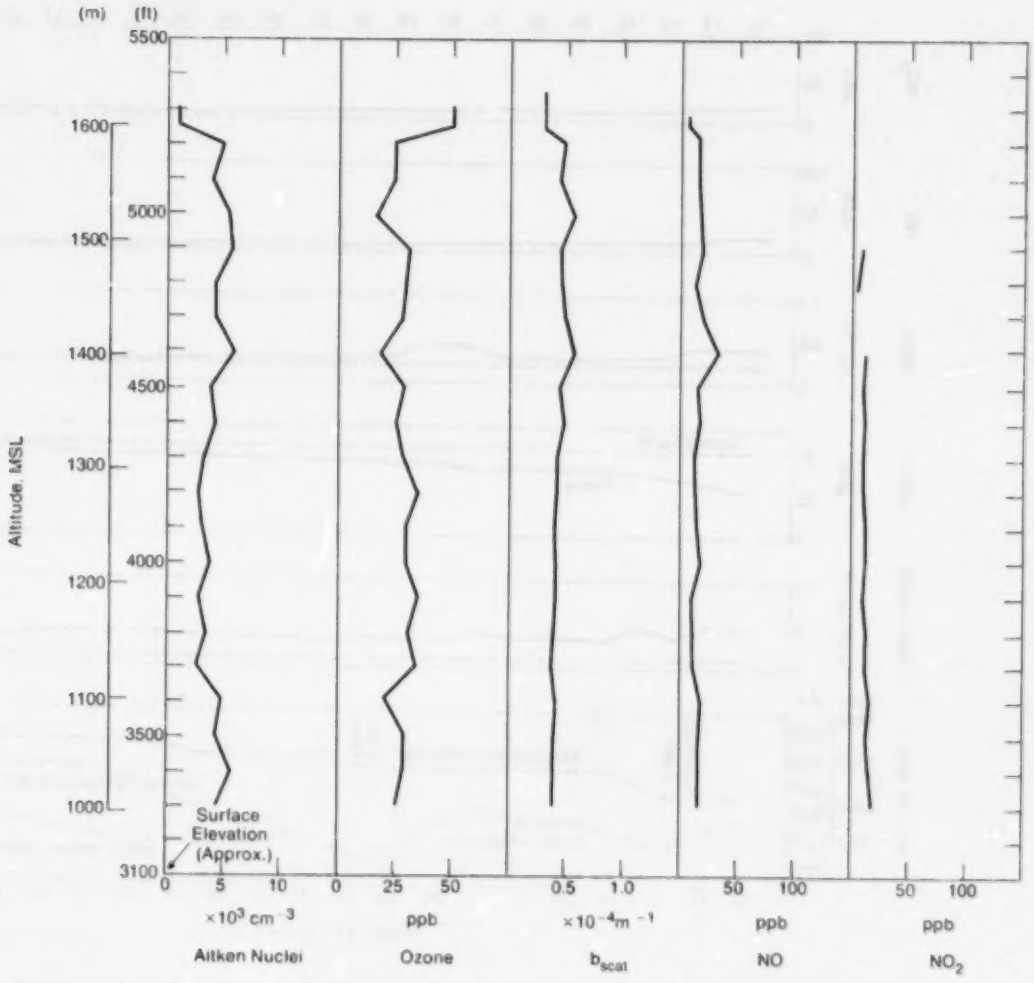

Figure 13. Plume constituent concentrations at the densest part of the plume during a vertical profile 12 km downwind, 31 August 77, 0915-1024 MDT.

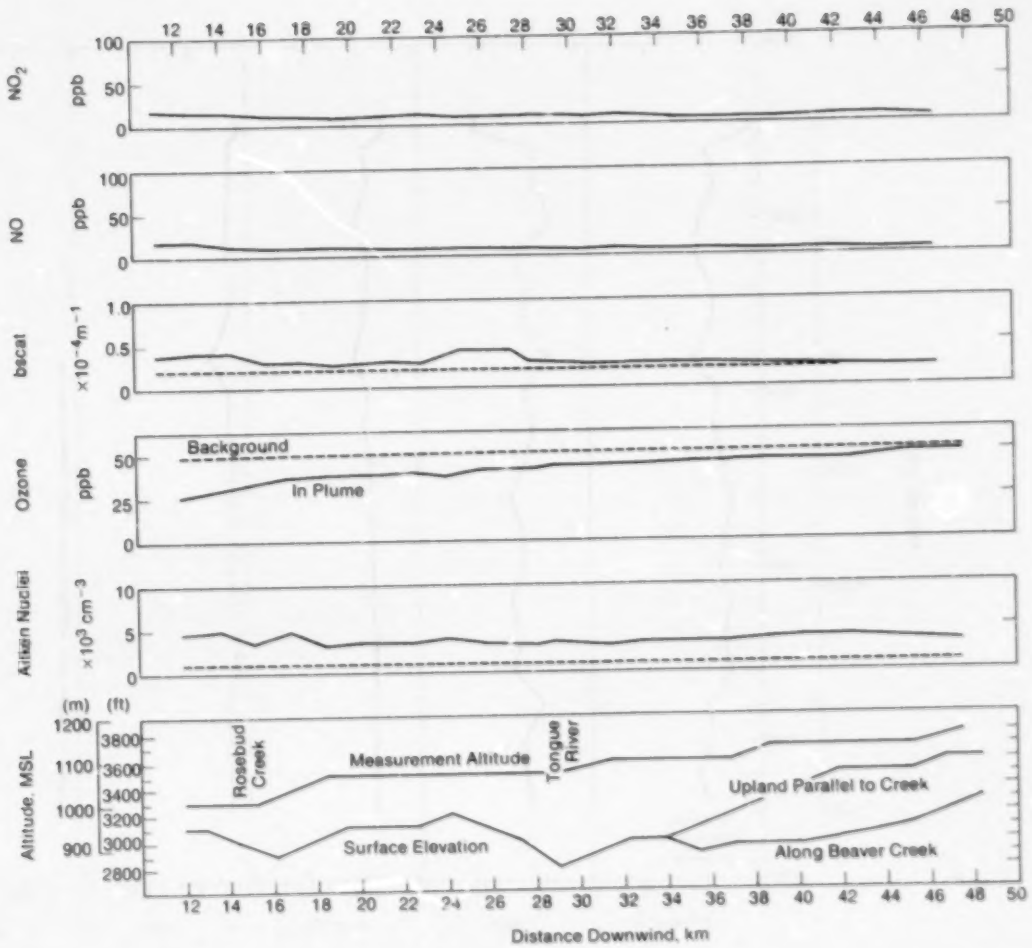

Figure 14. Plume constituent concentrations at the densest part of the plume, 31 August 77, 1024-1140 MDT; distance and altitude as indicated.

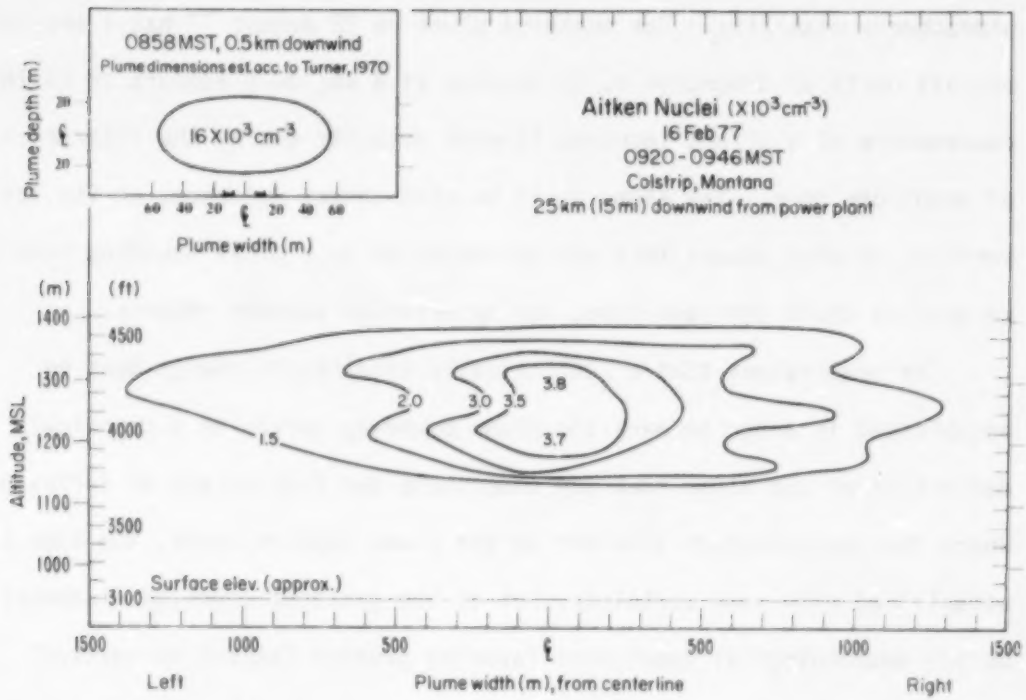

Figure 15. Vertical contour profile of the Colstrip plume 16 Feb 77, 0920-0946 MST; the inset represents the theoretical plume boundary and measured concentration. Plume traverses were done at 30 m (100 ft) intervals between 1130 m (3700 ft) and 1370 m (4500 ft) MSL. Plume constituents were not detected during the highest and lowest altitude crossings.

is apparent from Table 6 that theory usually understates the plume width. The predicted thicknesses are considerably larger than measured; the differences are probably a consequence of the extreme dependence of vertical extent on atmospheric stability. The measured plume on 28 August 77 has a smaller overall vertical dimension at 12 km than at 4 km; this appears to be the consequence of a slight increase in wind velocity during the intervening time of about one hour. The plume at 12 km also showed evidence, on its top surface, of wind shear; this was corroborated by a pibal sounding less than 2 km away at about the same time, and by aviation weather reports.

The requirement that a statistically significant change must be established in order to mark the plume boundary serves as a practical definition of the plume that may understate the true extent of diffusion. Where the concentration gradient at the plume edge is steep, the edge can be established with some certainty, but at the greatest downwind distances, and during meteorological conditions favoring greater lateral or vertical dispersion, the plume boundary location may be quite imprecise. An example may be seen in the horizontal plume profile of 1 September 77 (Figure 10) at downwind distances greater than 40 km. In this instance the plume's west edge was well defined, but concentrations on the east edge gradually tapered off to the instrumental noise level. In the vertical profiles of Figures 9, 11, and 15 the research aircraft made cross-plume passes, in direction normal to the plume axis, beginning above the plume and descending in 30 m (100 ft.) intervals, unless otherwise indicated. In the profiles of Figures 9 and 11 the bottom boundary of the plume was not located except by visual indication (Figure 9) or by the assumption of mixing to the surface (Figure 11).

The discrepancies between measured and calculated plume width are the results of at least three conditions: (a) our measurements with the mobile

laboratory at the Hay Coulee site 12 km SE of the Colstrip powerplant show wind direction commonly fluctuating over a range of 40° to 70°; (b) terrain factors in the vicinity of Colstrip contribute additional deflection of wind direction (see below); (c) neither AN nor ozone concentration is ideal for use as a plume tracer. Both are non-conservative in the sense that the profile dimensions and measured constituent concentrations indicate a reactive mixture involving a particle generating process; ozone reaction and particle generation were discussed earlier. In every example of Colstrip plume measurements where we measured concentrations of both substances the plume edges would have been identical, within the limits of experimental error, with O_3 always being depleted and AN always augmented. Thus, having chosen tracers of opportunity does not compromise our finding of a disagreement between measured and predicted plume width. In Table 6 two stability indexes, with the appropriate dimensions, are listed because some ambiguity exists regarding the correct designation.

5. Plume Trajectories

According to Hunt et al. (1979) and Brighton (1978), in neutral or stable stratified air flow around a hill the vertical motion and diffusion are negligible. Displacement occurs in the horizontal direction only, with laminar flow taking place upwind of and around the hill. In the wake region vortices may occur, but motion remains predominately horizontal. Reid (1979) described a study in the mountains of Colorado where transport and turbulent dispersion in the boundary layer were investigated. The local transport and dispersion processes in the mountain valleys were found to be highly complex, with a high frequency of shallow diabatic flow, strong terrain channeling of flow, and a high frequency of capping inversions.

Tracking of the Colstrip powerplant plume with the aircraft has, on

occasion, established plume trajectories that can best be explained by consideration of the underlying terrain. Measurements of the plume on three successive days during time of a neutral or slightly unstable atmosphere provided good examples of such situations; Figure 1 (U.S. Geological Survey, 1963) will assist the reader in following the descriptions of plume trajectories that follow.

Measurements of wind direction and velocity made at the Hay Coulee mobile laboratory site with continuous recording instruments were accepted as representative of wind direction at plume altitude in these instances, given the lack of suitable measurements at plume altitude.

(1) On 30 August 77 at 0615 MDT our research aircraft encountered the plume near Colstrip, followed it southeast about 13 km to the Rosebud Creek valley, then 18-20 km southwest along the valley to the vicinity of Lame Deer, thus establishing a direction of plume flow that was almost directly opposed to the wind direction as reported at Miles City, Montana, and at Hay Coulee. A vertical profile on the powerplant plume was constructed near Lame Deer from 0645 to 0735 MDT, and then the plume was followed 20-22 km farther southwest along the Rosebud Creek valley as far as the town of Busby. The profile plume edges and representation of approximate terrain contours are presented in Figure 16. Constituent concentrations in the densest part of the plume are shown in Figure 17. At 0600 MDT, the Miles City, Montana, airport reported surface wind of 3.6 m s^{-1} at 280°; winds at 6000 ft. (1829 m) MSL were 7 m s^{-1} at 270°. The surface record from our mobile laboratory at the Hay Coulee field site 12 km southeast of the powerplant shows the 0600 MDT wind at 260° and less than 2 m s^{-1}.

From approximately 2150 MDT, 29 August, to 0200 MDT, 30 August, the wind direction had been between 330° and 360° at Hay Coulee, with an apparent

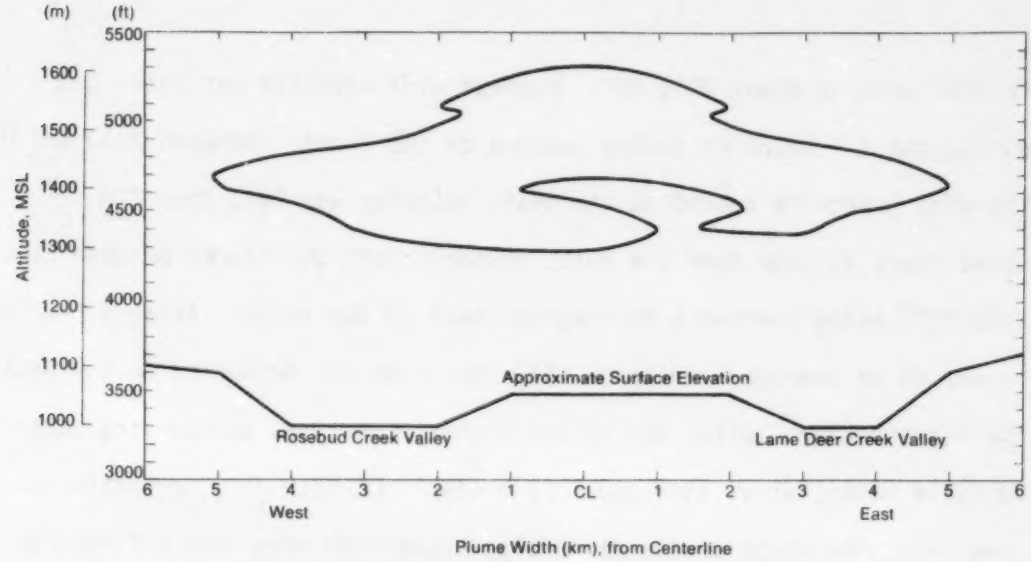

Figure 16. Vertical boundary profile of the Colstrip plume from Aitken nucleus concentrations on 30 August 77, 0645-0735 MDT, 29 km downwind (near Lame Deer).

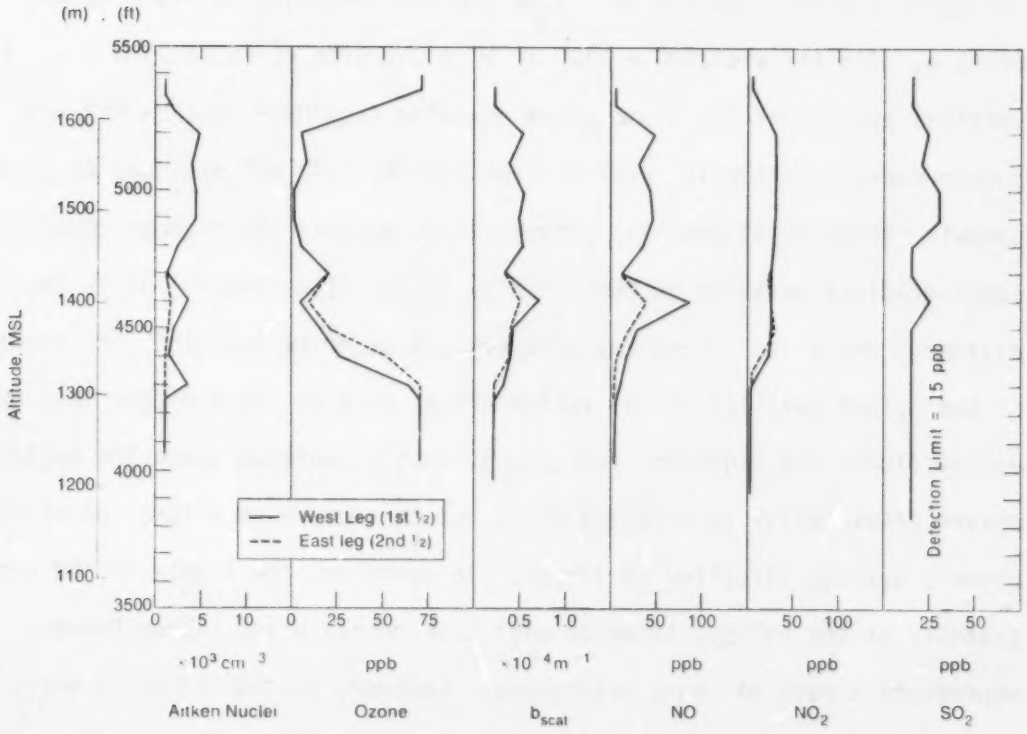

Figure 17. Plume constituent concentrations at the densest part of the Colstrip plume during a vertical profile on 30 August 77, 0645-0735 MDT, 29 km downwind (near Lame Deer).

frontal passage about 2300 MDT. Maximum wind velocity was about 8 m s^{-1} during the 1.5 hours following passage of the front. Between 2000 and 0600 the wind gradually backed to the west; velocity was less than 2 m s^{-1}. The plume found at Lame Deer and Busby probably left the stacks between 2150 and 0200 MDT, being carried a few degrees east of due south. After a few hours travel at an average heading of 165° the plume was deflected to the west by the Rosebud Creek valley and by the higher elevations surrounding Badger and Garfield Peaks, elev. 1348 and 1315 m (4422 and 4315 ft), respectively. Near Lame Deer, the shape of the plume also appears to have been affected by the valley of Lame Deer Creek, which flows into Rosebud Creek from the south.

(2) On 31 August 77, for several hours following 0800 MDT, the wind direction recorded at Hay Coulee was between 290° and 330°, with velocities averaging 5 m s^{-1}. During this time the wind recorded at stack height (1141 m, 3745 ft) was 290° - 330° at 10 m s^{-1} with gusts to 15 m s^{-1}. A vertical profile of the plume 12 km downwind from 0915 to 1024 MDT was constructed; a horizontal profile from 1024 to 1140 MDT was done 12 to 48 km downwind (Figures 11 and 12). Figure 13 summarizes the highest constituent concentrations measured in the vicinity of the plume centerline at the various distances downwind. Along Beaver Creek, 34 to 48 km downwind, the elevations of the upland parallel to the valley are as much as 150 m higher than the valley floor; the plume was found to be neatly centered along the valley. The Beaver Creek valley is oriented so as not to require an alteration of the plume's average direction of travel. In addition, the saddle at the upper boundary of the valley, lying between Cook Mountain and Liscom Butte, represents a path of least resistance. However, in the situation where the wind direction varies over a 40° range, the probability of the plume centering on Beaver Creek valley and the saddle without a ducting influence would have

been very low. Thus, we consider this to be an instance of ducting.

(3) On 1 September 77, winds at Hay Coulee at 1030 MDT were 320° ± 30°, with a gradual change in direction to 360° by 1400 MDT. Wind direction stayed constant at 360° until 1540 MDT, when it moved to 340° for 45 min. It then returned to 360° for most of the time until about 1900 MDT. Wind velocity, as measured at Hay Coulee, was 7 m s^{-1} at 1500 MDT. The research aircraft worked a vertical plume profile near Hay Coulee from 1233 to 1249 MDT. It then commenced a horizontal plume profile out to a distance of 45 km downwind, ending at 1500 MDT (Figures 9 and 10), several km southwest of Ashland in the Tongue River Valley. The approximate mean true heading of the plume was 160° from the plant past the Rosebud Creek valley, then 130° to an area east of Garfield Peak, 180-190° until the end of the flight. The net downwind progress rate of the aircraft during the horizontal profile was 4 m s^{-1}. Flight altitude was 1340 to 1370 m (4400 to 4500 ft.) MSL during that portion of the flight conducted northeast and east of the Badger and Garfield Peaks highland, i.e., the flight altitude was about the same as the elevation of the Peaks. The plume's west edge was well defined, and the plume was well separated laterally (not less than 2 km) from possible ground contact; this separation is regarded as a possible consequence of diabatic flow, i.e., of upslope air flow produced by solar heating of the surface such as to carry non-contaminated valley air up to plume elevation. The east edge of the plume was less well defined, and toward the conclusion of the flight, southwest of Ashland, no attempt was made to locate the eastern plume boundary. This latter part of the flight was made at 1250 to 1310 m (4100 to 4300 ft.) MSL, and lateral separation between the west plume edge and terrain was ~ 1 km. It appears here that the plume was deflected to the east around the Badger and Garfield Peaks highland, and then ducted slightly west of due south by the

Tongue River valley, or by horizontal displacement from vortex formation in the lee of the upland region (Brighton, 1978). The wind was neither westerly enough in the first instance, nor north-easterly enough in the latter to have caused such a plume trajectory. In short, the evidence indicates a deflection in the direction of plume travel by 20° or more from the prevailing wind direction, as measured at Hay Coulee.

Measurements of gases and particles in the plume of the Colstrip, MT coal-fired powerplant showed transport and diffusion patterns that are not manageable with existing models. Terrain elevations south and southeast of the plant that are less than 300 m (1000 ft.) higher than the altitude of plume emission were found to have a marked influence on plume transport by causing substantial deviation from the apparent prevailing wind direction as recorded at Hay Coulee and/or at stack height near the plant. The work reported here is in rough agreement with the model-derived conclusions of Hunt et al. (1979) and Brighton (1978) that primarily horizontal motions occur in neutral or stable stratified flow around an obstacle.

6. Particle Composition

Figures 18 and 19 show the SEM-EDX analyses of some filter samples collected in Hay Coulee or in the vicinity on 27 and 29 May 1977. In each case 75 particles were analyzed, except in air #5b on 29 May 1977, which was a very lightly loaded background sample. Of the 75 particles analyzed, 30 were in the size range of 0.1 - 0.4 μm diameter. In addition to elemental analyses, the particles were classified according to size (0.1-0.4 μm, and 1.5-10 μm) and shape (spherical or irregular). The 27 May 1977 Ground #1 and Air #1 samples are very similar; both represent background air. The high proportion of spherical particles is not common in background samples, but is seen occasionally, and is regarded either as the product of condensation of

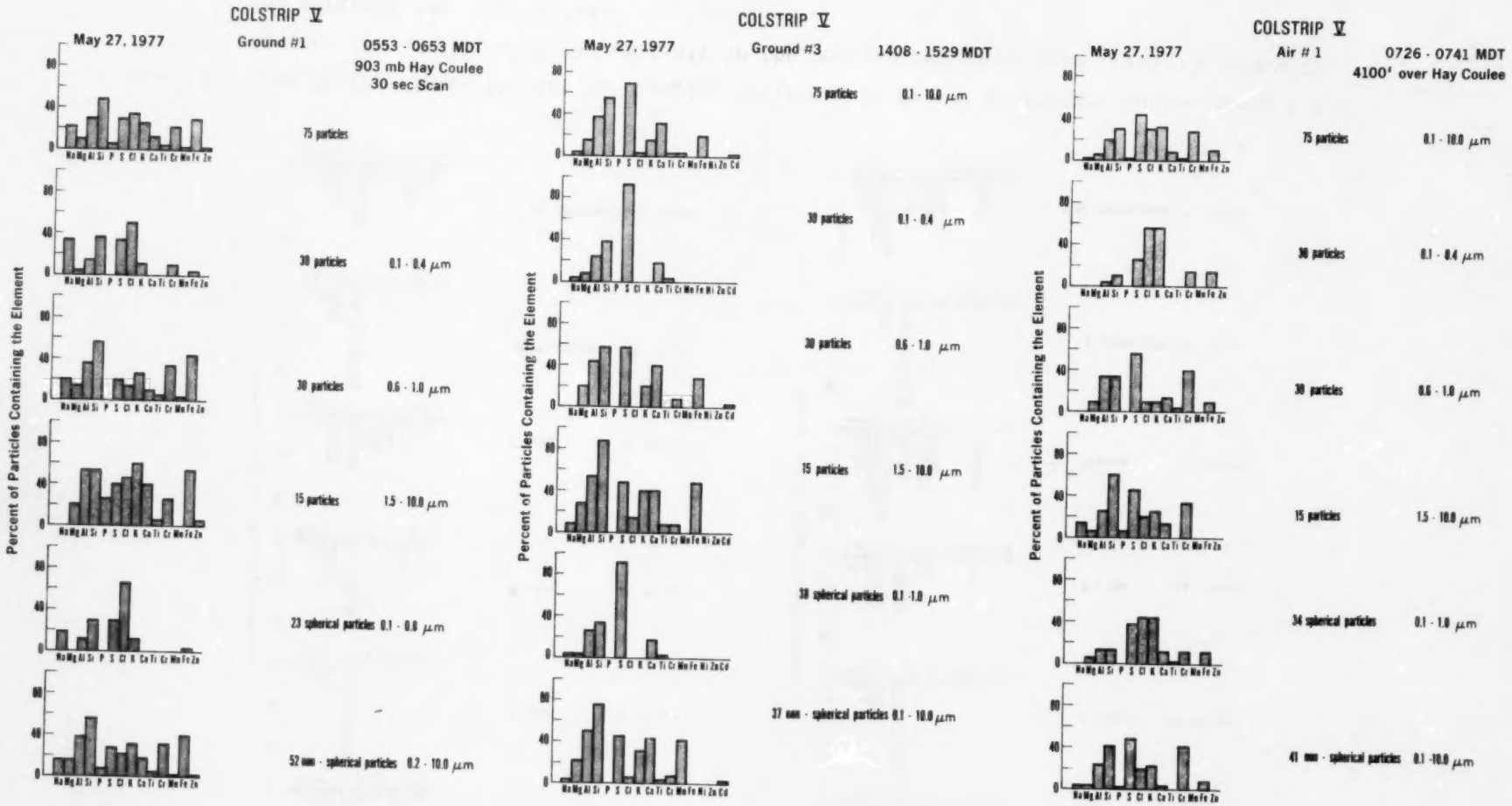
COLSTRIP V
May 27, 1977
Ground #1
0553 - 0653 MDT
903 mb Hay Coulee
30 sec Scan
Percent of Particles Containing the Element
75 particles
30 particles 0.1 - 0.4 μm
30 particles 0.6 - 1.0 μm
15 particles 1.5 - 10.0 μm
23 spherical particles 0.1 - 0.8 μm
52 non - spherical particles 0.2 - 10.0 μm
COLSTRIP V
May 27, 1977
Ground #3
1408 - 1529 MDT
75 particles 0.1 - 10.0 μm
30 particles 0.1 - 0.4 μm
30 particles 0.6 - 1.0 μm
15 particles 1.5 - 10.0 μm
38 spherical particles 0.1 -1.0 μm
37 non - spherical particles 0.1 - 10.0 μm
COLSTRIP V
May 27, 1977
Air # 1
0726 - 0741 MDT
4100' over Hay Coulee
75 particles 0.1 - 10.0 μm
30 particles 0.1 - 0.4 μm
30 particles 0.6 - 1.0 μm
15 particles 1.5 - 10.0 μm
34 spherical particles 0.1 - 1.0 μm
41 non - spherical particles 0.1 -10.0 μm

Figure 18. SEM-EDX derived classification of aerosol samples collected on membrane filters that were collected at the Hay Coulee field site and with the aircraft over Hay Coulee on 27 may 77. The top bar graph shows the elemental occurrence in the 75 particles that were examined. The next three graphs, reading downward, show elemental occurrence in the particles as classified according to particle diameter. The bottom two graphs show elemental occurrence in the particles as classified according to particle shape; the inclusive size ranges are shown for all particles in these two shape classifications.

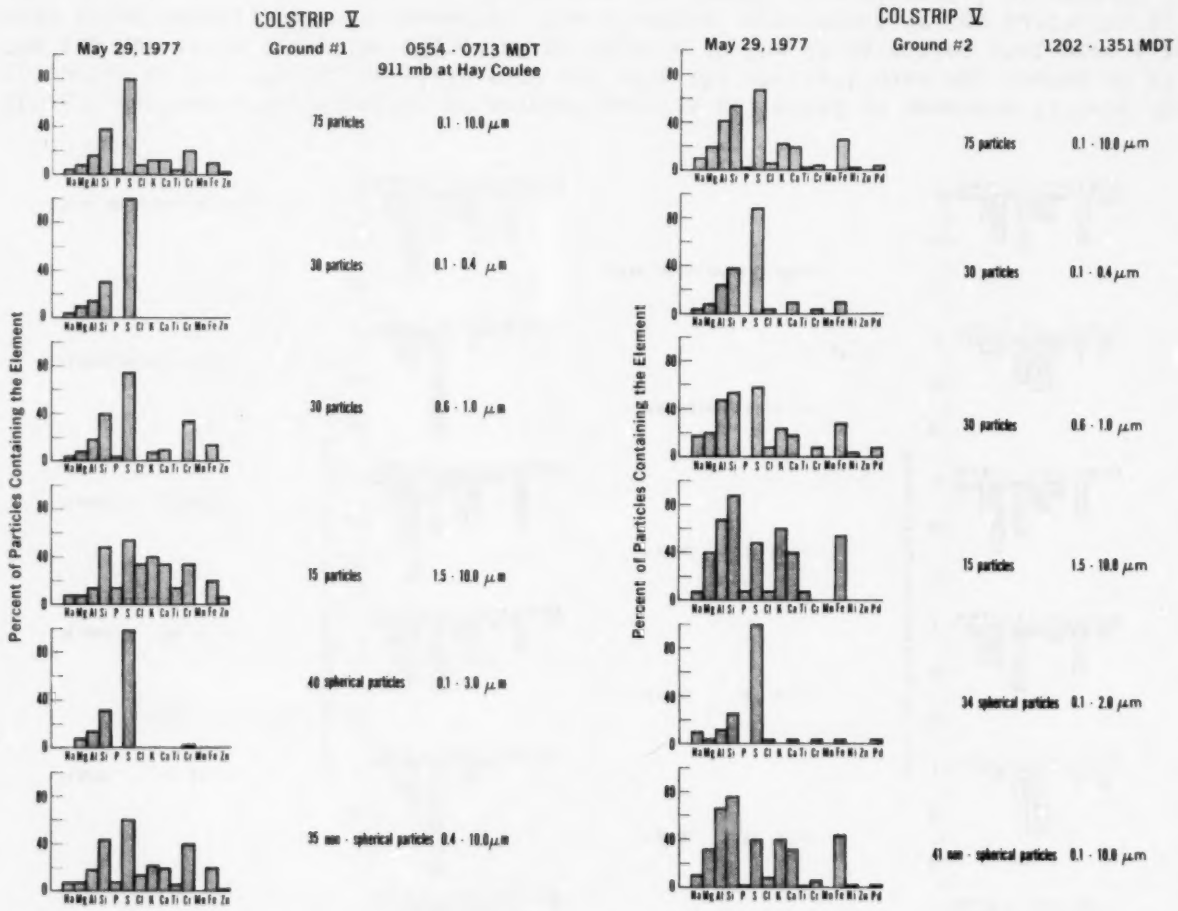
COLSTRIP V
May 29, 1977
Ground #1
0554 - 0713 MDT
911 mb at Hay Coulee
75 particles 0.1 - 10.0 μm
30 particles 0.1 - 0.4 μm
30 particles 0.6 - 1.0 μm
15 particles 1.5 - 10.0 μm
40 spherical particles 0.1 - 3.0 μm
35 non - spherical particles 0.4 - 10.0 μm
Percent of Particles Containing the Element
COLSTRIP V
May 29, 1977
Ground #2
1202 - 1351 MDT
75 particles 0.1 - 10.0 μm
30 particles 0.1 - 0.4 μm
30 particles 0.6 - 1.0 μm
15 particles 1.5 - 10.0 μm
34 spherical particles 0.1 - 2.0 μm
41 non - spherical particles 0.1 - 10.0 μm
Percent of Particles Containing the Element

Figure 19. Same as for Figure 18, but for samples collected 29 May 77 at the Hay Coulee field site (Ground #1 and #2), with the aircraft in the power plant plume near Colstrip, and with the aircraft over Hay Coulee.

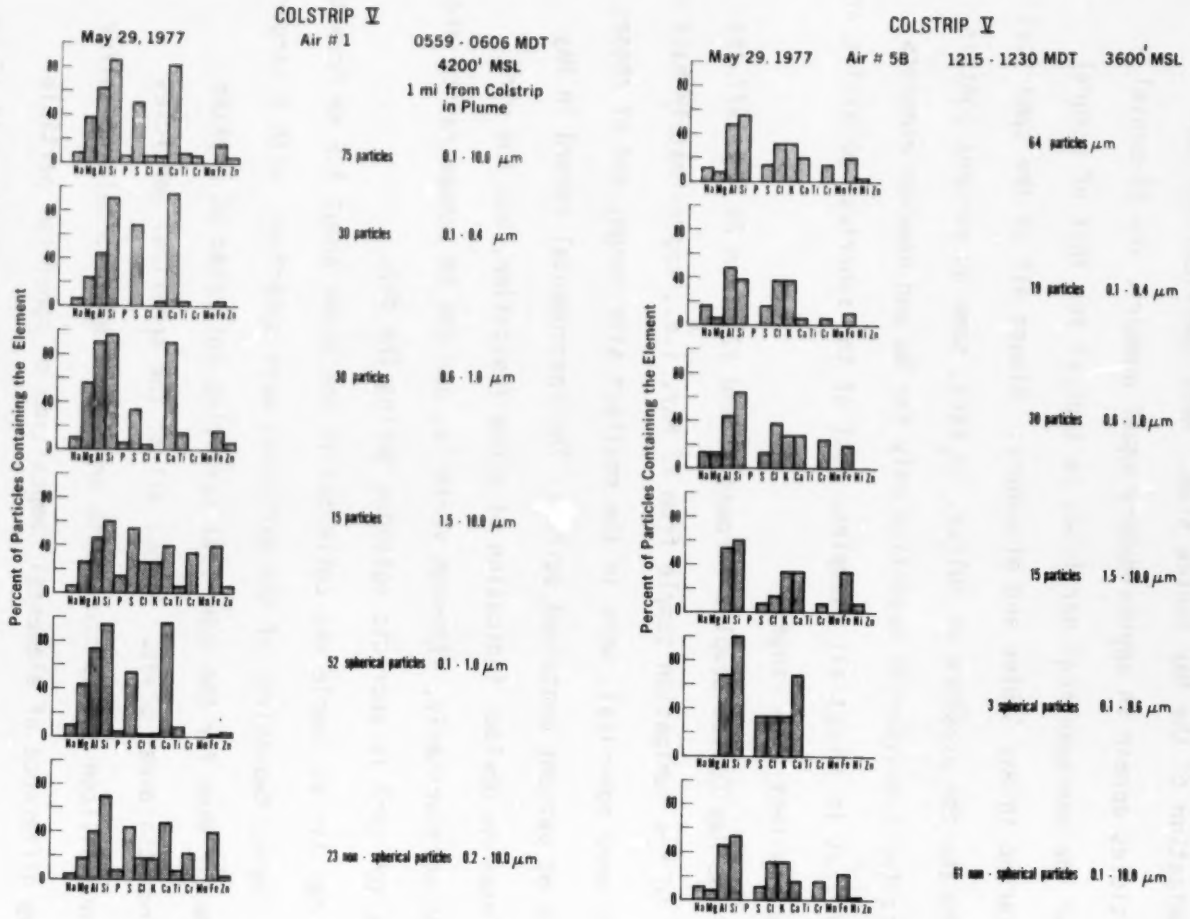
COLSTRIP V
May 29, 1977
Air # 1
0559 - 0606 MDT
4200' MSL
1 mi from Colstrip in Plume
75 particles 0.1 - 10.0 μm
30 particles 0.1 - 0.4 μm
30 particles 0.6 - 1.0 μm
15 particles 1.5 - 10.0 μm
52 spherical particles 0.1 - 1.0 μm
23 non - spherical particles 0.2 - 10.0 μm
Percent of Particles Containing the Element
Na Mg Al Si P S Cl K Ca Ti Cr Mn Fe Zn
COLSTRIP V
May 29, 1977
Air # 5B
1215 - 1230 MDT
3600' MSL
64 particles μm
19 particles 0.1 - 0.4 μm
30 particles 0.6 - 1.0 μm
15 particles 1.5 - 10.0 μm
3 spherical particles 0.1 - 0.6 μm
61 non - spherical particles 0.1 - 10.0 μm
Percent of Particles Containing the Element
Na Mg Al Si P S Cl K Ca Ti Cr Mn Fe Ni Zn

Figure 19. (Continued)

biological materials or the diluted remnant of combustion emissions from an unidentifiable source or sources. The 27 May Ground #3 sample was collected during the fumigation of the Hay Coulee site. Here spherical and non-spherical particles appear in approximately equal numbers. The elemental composition of the non-spherical particles is typical for that of natural aerosols collected in Hay Coulee and elsewhere. Almost all of the spherical particles indicate the presence of sulfur, in fact, some 60 percent contain nothing but sulfur (considering detection only for Na and heavier elements). In this sample, as in almost all examples, most of the spherical particles are formed in the smallest size range.

Both of the Hay Coulee samples (Ground #1 and #2) from 29 May 1977 are very similar to the fumigation sample from 27 May, i.e., approximately half of the particles were spherical, were in the smallest size range, and of these, approximately 60 percent contained sulfur. The instrumental record in Hay Coulee disclosed no obvious indication of plume fumigation, but the wind direction was northwesterly, although variable, and the AN concentration did exceed 1.2×10^4 cm^{-3} in sporadic episodes during the day.

The 29 May Air #1 sample was collected in the plume about 1.6 km from the powerplant. Here, two-thirds of the particles were spherical, with a larger average diameter than for the spherical particles collected at greater distances from the power plant. Almost all of the spherical particles contained both silicon and calcium, with only about half containing sulfur. The striking difference of elemental composition of spherical particles collected at 1.6 km downwind, as compared with that at a distance of 12 km shows that the particles in the plume at the shorter distance had, for the most part, settled out by the time (1 - 3 h) that part of the plume reached Hay Coulee, and the glassy mineral spheres had been replaced by sulfate

particles resulting from sulfur dioxide oxidation.

Several samples collected with the research aircraft in February and March 1979 were analyzed with an automated SEM-EDX. In this case many more particles were analyzed, usually about 500, but the detection and elemental classification parameters excluded most of the sulfate-containing particles of diameter < 0.2 μm. Thus, the sulfur analyses shown in Figures 20, 21 and 22 should be regarded as a lower limit or ignored, and analyses for the other 21 elements should be considered only as relating to particles of diameter > 0.2 μm. Figures 21 and 22 include relative signal strength, indicating elemental abundance as well as distribution. Thus, in Figure 21 where 47 percent of the emitting particles contain silicon, the X-ray emissions due to silicon account for 34 percent of all X-ray emissions; 72 percent of emitting particles contain calcium, but calcium emissions account for only 15 percent of the total emissions; and 9 percent of emitting particles contain iron, but iron emissions account for 30 percent of total emissions. We see that calcium is rather widely distributed in the plume particles at this distance from the stacks, but nevertheless is apparently only a minor constituent, whereas iron occurs in a few particles, but these few particles must be large and/or composed primarily of iron.

In the samples of Figure 20 the elemental composition is like fly ash; calcium is prominent, especially at the shorter distances, as would be expected from this lime-scrubbed plume. Some of the differences seen from sample to sample may be due to differences in coal or soil composition. Twelve samples collected during 1977 and 1979 were analyzed for the 22 elements shown in Figure 21; of these, eight contained uranium in trace concentrations. All samples consisted of > 50 percent spherical particles; plume and background samples were the same in this respect.

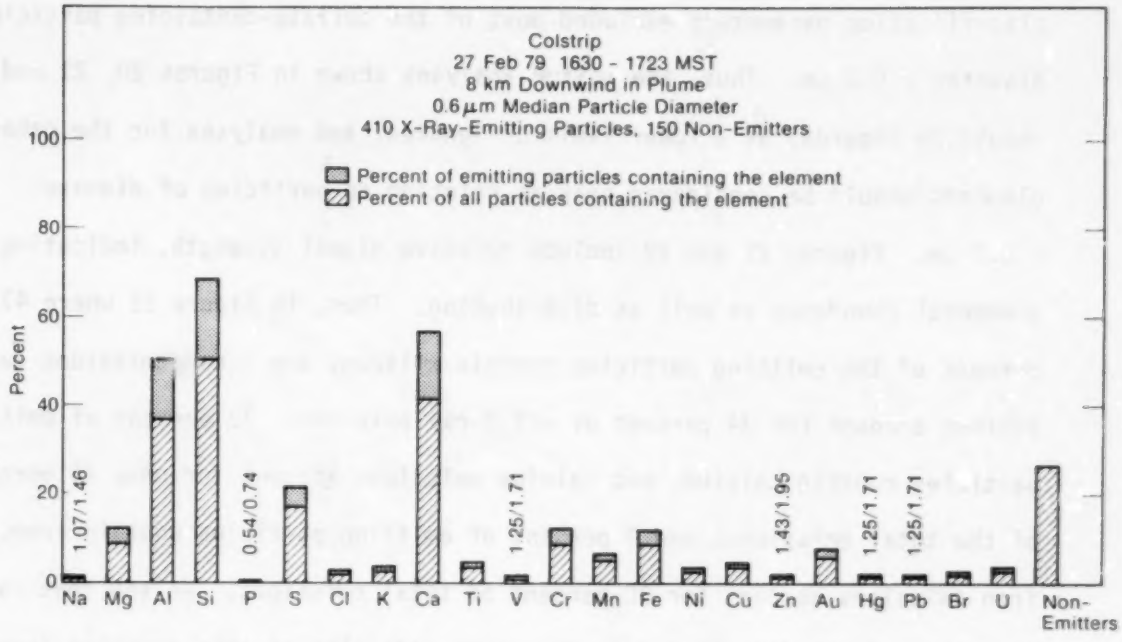

Figure 20. SEM-EDX analysis of particles collected on Nuclepore filters, 27 February 79, 1630-1723 MST. Numbers appearing above the very short bars indicate the percent of particles containing the element.

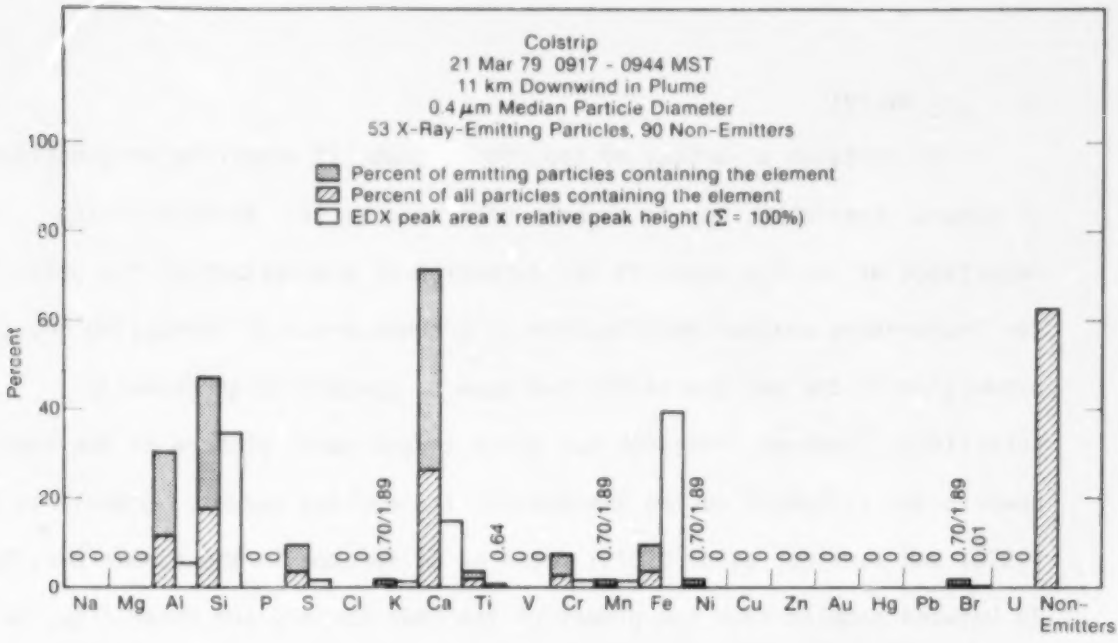
Colstrip
21 Mar 79 0917 - 0944 MST
11 km Downwind in Plume
0.4 μm Median Particle Diameter
53 X-Ray-Emitting Particles, 90 Non-Emitters
Percent of emitting particles containing the element
Percent of all particles containing the element
EDX peak area x relative peak height (Σ = 100%)
Percent
0.70/1.89
0.64
0.70/1.89
0.70/1.89
0.70/1.89
0.01
Na Mg Al Si P S Cl K Ca Ti V Cr Mn Fe Ni Cu Zn Au Hg Pb Br U Non-Emitters

Figure 21. SEM-EDX analysis of particles collected on Nuclepore filters, 21 March 79, 0917-0944 MST. EDX peak area times relative peak height indicates emission strength and thus indicates the relative concentration of the element in the sample.

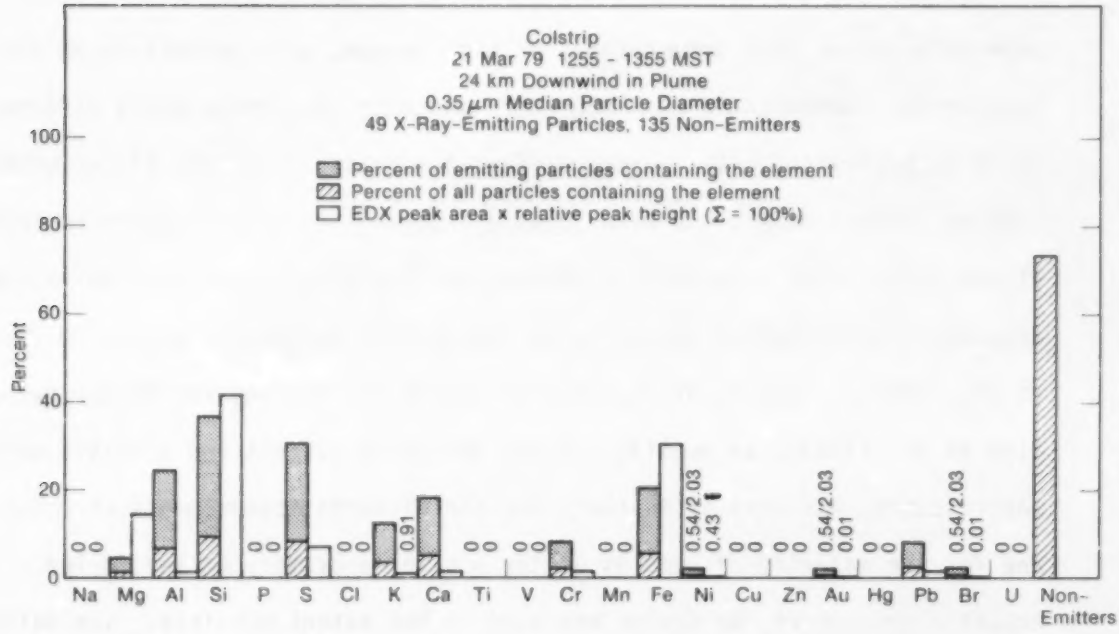
Colstrip
21 Mar 79 1255 - 1355 MST
24 km Downwind in Plume
0.35 μm Median Particle Diameter
49 X-Ray-Emitting Particles, 135 Non-Emitters
Percent of emitting particles containing the element
Percent of all particles containing the element
EDX peak area x relative peak height (Σ = 100%)
Percent
0.91
0.54/2.03
0.43
0.54/2.03
0.01
0.54/2.03
0.01
Na Mg Al Si P S Cl K Ca Ti V Cr Mn Fe Ni Cu Zn Au Hg Pb Br U Non-Emitters

Figure 22. SEM-EDX analysis of particles collected on Nuclepore filters, 21 March 79, 1255-1355 MST. The numbers above very short bars indicate the percent of particles containing the element. EDX peak area times relative peak height indicates emission strength and thus indicates relative concentration of the element in the sample.

7. Ice Nuclei

Coal contains a variety of impurities that, if occurring as constituents of aerosol particles, may be capable of acting as IN. Because of the importance of the ice phase in the formation of precipitation, the potential for inadvertent weather modification as a consequence of increasing energy production in the western states has been of concern to atmospheric scientists. However, research has given an ambiguous picture of the impact of power plant effluents on the atmospheric ice nucleus budget. Schnell et al. (1976) and Pueschel et al (1979) found no difference in the number density of IN between samples from the plumes of the Four Corners and Homer City, PA power plants and samples of the surrounding clean air. Parungo et al. (1978) found similar results when samples were handled in a manner similar to that described by Schnell et al.; however, Parungo et al. discovered that IN could be activated in the plume samples by subjecting the sample to high water supersaturation, high temperature, or high vacuum, or combinations of these treatments. Research in our laboratory suggests that tests using different modes of nucleation will produce different results, i.e., the filter method used by Schnell et al. and Parungo et al. depends upon the deposition (reverse of sublimation) or condensation-followed-by-freezing mechanisms, while the acoustic counter method depends upon the contact nucleation mechanism (Langer et al., 1967). Because of its ease of sample collection, the filter method of Bigg et al. (1963), as modified to use Nuclepore filters and a static water vapor source, was used exclusively for the airborne measurements at Colstrip, and for the majority of samples at the mobile laboratory at Hay Coulee. The acoustic counter at Hay Coulee was used to the extent possible. Van Valin et al. (1979) showed that the ice nucleus concentration, as measured by the acoustic counter method during a well-documented plume exposure at Hay Coulee

(Figure 23), was raised by nearly an order of magnitude. Similar episodes of plume exposure at Hay Coulee, while not always as striking, produced similar increases in the IN-acoustic counter method (Table 7). During times of non-exposure to the plume this method showed IN concentrations in the range 1-4 ℓ^{-1}. However, filter-method samples collected during these times of plume exposure were not different from those collected during non-exposure times. Hay Coulee filter-method ice nucleus measurements for the four field periods in 1976 and 1977 are listed in Table 8. In addition to the comparison of IN concentrations between plume and non-plume exposures, the samples were segregated by time of collection (morning, mid-day, and afternoon), but the variability is so large that one cannot have confidence in a possible pattern. In like manner, the plume and ambient atmosphere samples cannot be shown to be different; the present methods are not sufficient to identify the plume as a source of IN. The filter-method (modified from Bigg et al., 1963) IN measurements of samples collected with the aircraft are presented in Table 9. Again, no difference can be shown between the plume and ambient IN concentrations.

The indication that IN were not generated during operation of coal-fired power plants has caused some puzzlement and skepticism. Parungo et al. (1978), using the same acoustic IN counter, measured very much higher IN concentrations during plume exposure periods and also observed enhanced snowfall downwind from a power plant near Boulder, Co. However, Hobbs et al. (1980), using a similar acoustic IN counter in their research aircraft, found no elevation of IN in the plume from the Centralia, WA power plant. Such apparently conflicting results, along with the variations in "background" concentration reported (e.g., this work; Schnell et al., 1976; Hobbs et al., 1980), sharpen the sense of uncertainty about the measurement of IN.

Table 7.--AEROSOL PARAMETERS MEASURED AT HAY COULEE SITE, 20 AUGUST to 3 SEPTEMBER, 1977.

Date	Elevated CN Concen. Begin	End	AN Max. Concen. ($\times 10^3 cm^{-3}$)	Character of CN Elevation	Wind Direction	Wind Velocity $msec^{-1}$	Other, Time of Measurements	CN, Avg. Concen. ($\times 10^3 cm^{-3}$)	b_{scat} ($\times 10^{-4} m^{-1}$)	CCN No. of Meas.	CCN Avg. (cm^{-3})	IN Filter No. of Meas.	IN Method Concen. (ℓ^{-1})	IN Acoustic Concen. (ℓ^{-1})
P 8-20	2100	2400	6.8	Intermittent	calm									
8-21	0000	0630	7.8	Continuous, steady, gradually declining	calm									
8-21							0855-1025	2.2				1	3.1	
P 8-21	1200	1700	24.0	Continuous, lg. variation	N	3				5	602 ± 295	2	2.3	>10
8-21	2240	2400	4.1	Continuous, variable	calm									
8-22	0000	0200	7.3	Continuous, steady, declining gradually	calm									
8-22	0345	0430	5.0	Continuous, steady	calm									
8-22					NNE	4	0622-1110	1.9		4	472 ± 258	2	10.3	
P 8-22	1406	1515	20.0	Continuous, several pulses	N	3				4	577 ± 231	1	7.8	
P 8-22	2107	2230	10.0	Continuous, several pulses first	calm									
P 8-23	0828	0854	48.0	Many strong pulses	NW	2				2	1260	1	5.5	>10
P 8-23	1000	1010	10.0	Weak pulses	N	3								
8-23	1040	1900	28.0	Continuous, steady	N,NE	3				14	1130 ± 494	2	5.4	2.0
8-24	0800	0900	8.0	Gradual rise & fall	SW	2				2	525			2.0
8-24							1010-1155	2.6		4	578 ± 372			
8-24	1820	2120	7.8	Continuous, steady	NW	<2				4	385 ± 305	1	8.6	
8-25	0020	0120	5.1	Continuous, steady	NNW	7								
P 8-25	0636	0639	8.8	Weak pulses	WNW	3	3					1	1.6	
P 8-25	0810	0900	8.5	Continuous, variable	N	6				2	490			
P 8-25	1009	1047	10.0	Continuous, variable	NNW	4				2	460			
8-25	1058	1730	46.0	Continuous, variable thunderstorm @ 1730	variable gusty					5	434 ± 264	2	6.6	4.0
8-26	0000	0940	8.0	Continuous, steady	lt & variable					3	1190	1	3.8	
8-26							1000-2400	2-3				1	2.7	
8-27							1235-1445	2.0	.6	6	338 ± 205			
P 8-27	1500	1530	4.4	Continuous, variable	WNW	3			.48	2	840			

Table 7.--(continued)

Date	Elevated CN Concen. Begin	End	AN Max. Concen. (x $10^3 cm^{-3}$)	Character of CN Elevation	Wind Direction	Wind Velocity $msec^{-1}$	Other, Time of Measurements	CN, Avg. Concen. ($x10^3 cm^{-3}$)	b_{scat} (x $10^{-4} m^{-1}$)	CCN No. of Meas.	CCN Avg. (cm^{-3})	IN Filter No. of Meas.	IN Method Concen. (ℓ^{-1})	IN Acoustic Concen. (ℓ^{-1})
P 8-27	1653	1725	5.3	Continuous, variable	N	6(G18)			.48					
8-27							1800-2000	1.0	.47					
P 8-27	2230	2300	7.6	Continuous, variable	W	<2			.45					
8-28							0200-0600	1.5	.50					
8-28							0805-1145	2.8	.51	18	560 ± 206			
8-28	1310	1500	10.0	Continuous, steady	lt. & variable				.65	2	500	1	5.3	
8-28							1800-2400	2.0	.51					
8-29							1300-1600	3.0	.60	4	525 ± 185			
P 8-29	1605	1830	15.0	Continuous, variable	NNW	4			.65	6	1162 ± 379	1	3.5	10
8-29	1830	2300	10.0	Continuous, steady	lt. & variable				.52					
8-30							0200-0600	1.5	.50					
8-30							0825-1720	3.0	.55	14	535 ± 304			
P 8-30	1840	1905	8.0	Intermittent	NW	10			.55	2	1470			
P 8-30	2030	2120	6.5	Intermittent	NNW	8			.55					
8-31							0400-0600	1.8	.51					
8-31							0720-1445	2.6	.57	12	478 ± 191	2	10.4	
P 8-31	1530	1655	6.0	Intermittent	NW	3			.58	2	810			10
9-1							0200-0400	0.8	.55					
P 9-1	1000	1057	6.4	Continuous, variable	NW	4			.58	2	600			>10
P 9-1	1113	1234	11.1	Continuous, variable	NNW	6			.55	2	910			>10
P 9-1	1448	1830	6.3	Intermittent	NNW	4			.58	6	630 ± 153	1	4.6	>10
9-1	2200	2400	6.9	Continuous, steady	lt. & variable				.65					
9-2	0000	0600	7.4	Continuous, steady, ground fog	calm				.75					
9-2							0720-1210	2-3	.60	2	770	2	4.7	
9-3							0000-0600	1.8	.62					
P 9-3	1043	1200	19.2	Continuous, variable	NNW	<2			.70			1	9.7	
P 9-3	1300	1445	15.0	Continuous, variable	NNW	<2			.65					

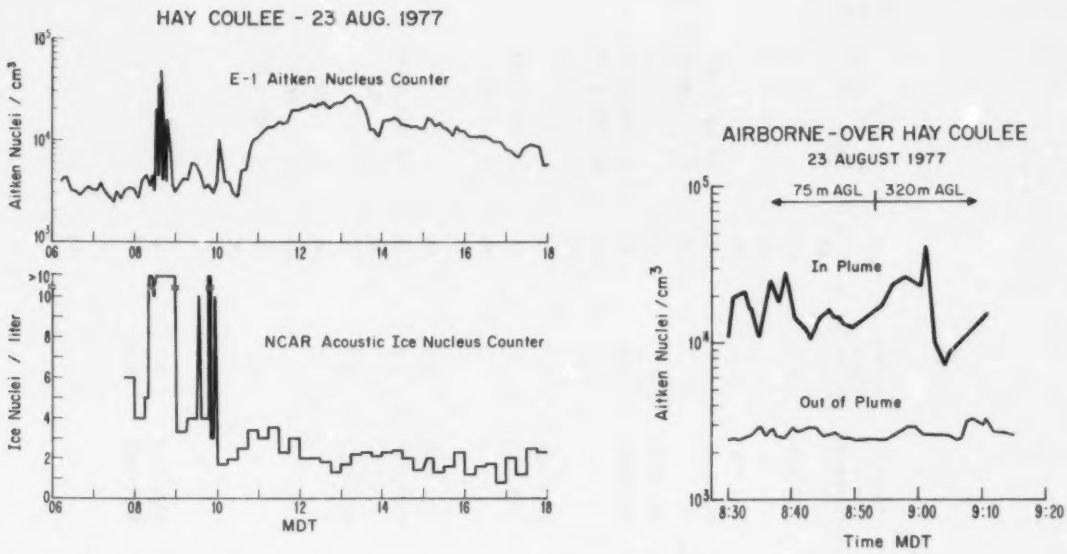

Figure 23. (Left) CN and IN concentrations measured at Hay Coulee showing power plant plume exposure from 0828 to 0854 MDT, and from 1000 to 1010 MDT.
(Right) CN concentration measurements with the aircraft during the time of the Hay Coulee plume exposure. The elevation of the Hay Coulee site is 930 m MSL.

Table 8.--ICE NUCLEUS CONCENTRATIONS (ℓ^{-1}) AT HAY COULEE AS MEASURED BY THE FILTER METHOD, EXPRESSED AS MEANS AND ONE-SIGMA STANDARD DEVIATIONS

Period	All samples	Before 1000 MDT	1000-1300 MDT	After 1300 MDT
May-June 76	(n=34) 2.03±1.63	(n=9) 3.67±1.42	(n=13) 1.80±1.64	(n=12) 1.07±0.58
Aug-Sept 76	(n=45) 2.78±1.15	(n=17) 3.12±1.15	(n=17) 2.54±1.27	(n=11) 2.62±0.91
May-June 77	(n=44) 2.43±1.56	(n=22) 2.83±1.53	(n=11) 2.58±1.89	(n=11) 1.54±0.75
Aug-Sept 77	(n=44) 6.43±3.59	(n=15) 7.74±5.00	(n=11) 5.87±3.08	(n=18) 5.68±2.02

Period	In Plume (all times)	Ambient (all times)
May-June 76	---	---
Aug-Sept 76	---	---
May-June 77	(n=9) 3.21±2.16	(n=35) 2.24±1.32
Aug-Sept 77	(n=10) 4.64±2.54	(n=34) 6.96±3.71

Note: n is the number of samples.

Table 9.--ICE NUCLEUS CONCENTRATIONS (ℓ^{-1}) FROM AIRBORNE SAMPLE COLLECTION AS MEASURED BY THE FILTER METHOD, EXPRESSED AS MEANS AND ONE-SIGMA STANDARD DEVIATIONS.

Period	In Plume	Ambient
May-June 76		(n=14) 0.88±0.60
Aug-Sept 76	(n=3) Ave = 2.56	(n=38) 1.19±1.02
Feb 77	(n=5) 1.36±0.31	(n=5) 0.93±0.34
May-June 77	(n=7) 1.58±0.68	(n=48) 1.61±1.29
21-25 Aug 77	(n=2) Ave = 3.04	(n=19) 2.07±1.96
27 Aug-2 Sept 77	(n=14) 4.56±4.06	(n=7) 7.30±5.26
Aug-Sept 77 (all flights)	(n=16) 4.37±3.82	(n=26) 3.48±3.87

Note: n is the number of samples

Nevertheless, much of the evidence indicates that the filter method used in this study is adversely affected by the surface absorption of substances, probably soluble sulfates, that deactivate the deposition and condensation-followed-by freezing modes of nucleation. The contact mode of nucleation is therefore affected to a significantly smaller degree. Further research on the ice-nucleating characteristics of plume aerosols continues.

8. Cloud Condensation Nuclei

Aerosol particles that can absorb moisture and form water droplets at supersaturations such as found in natural clouds are known as cloud condensation nuclei (CCN). During the 1975, 1976 and 1977 field projects of ACP, CCN average concentrations in the natural atmosphere in the vicinity of Colstrip were 6-700 cm^{-3}, and were seen to vary by a factor of about 3 (Van Valin and Pueschel, 1978, and Table 7). During periods of plume exposure, as measured during the August-September 1977 field project, the average CCN concentration was about twice that value. The CCN determinations are measurements of spot samples; because of the very changeable pollutant concentrations measured during a plume strike at Hay Coulee one must assume that the average value consists of both near-maximum and near-minimum concentration samples. The CCN concentrations changed very little during most 24-hour periods, excepting plume strike episodes, but CN concentrations were found to increase by as much as an order of magnitude during hot, sunny days (Figures 24 and 25). The CN were assumed to be organic, to be the product of gas-to-particle conversion of emissions from vegetation at the Hay Coulee site, and to be sized below the optical range, i.e., $r < 0.1$ μm. The increase of CCN concentration in the plume is probably due to both hygroscopic nitrate-containing particles and sulfate-containing particles of $r > 0.01$ μm). Naturally occurring CCN are probably particles containing soluble sulfates or

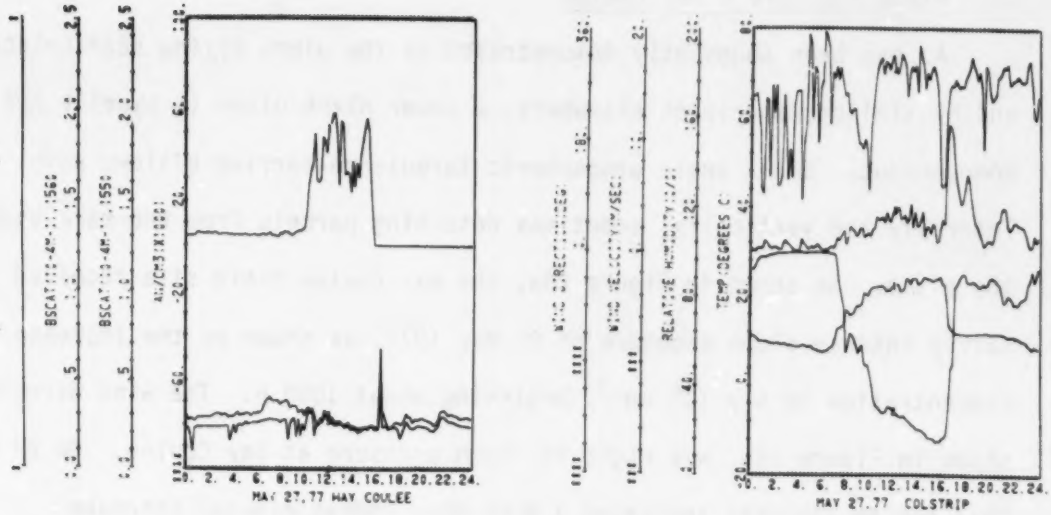

Figure 24. Continuously measured parameters at Hay Coulee, 27 May 77. Reading from left to right, the ordinates refer to plots numbered 1, 2, 3 and 4. The abscissa shows Mountain Daylight Time.

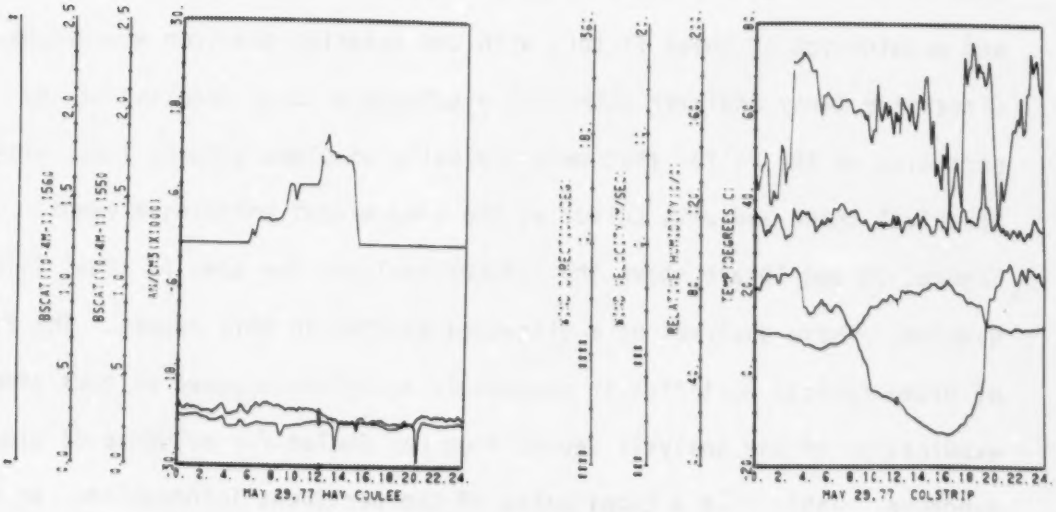

Figure 25. Record for Hay Coulee for 29 May 77.

chlorides (see Section 6).

9. Plume Exposure - Hay Coulee

As has been abundantly demonstrated by the plume flying near Colstrip, and by similar experience elsewhere, a power plant plume is usually not homogeneous. Small scale atmospheric turbulence carries billows both laterally and vertically, sometimes detaching parcels from the main body of the plume. As shown in Figure 24a, the Hay Coulee field site received a fairly intense plume exposure on 27 May 1977, as shown by the increase in AN concentration to 6 x 10^4 cm^{-3}, beginning about 1000 h. The wind direction, shown in Figure 24b, was right for such exposure at Hay Coulee. On 29 May 1977 the AN analysis indicated a much more modest mid-day increase (Figure 25a) that we had come to associate with biologically derived materials following daytime sun and temperature exposure; the wind direction was too southerly (Figure 25b) to expect plume exposure. Nuclepore filter samples were collected at Hay Coulee and in the aircraft in the vicinity of Hay Coulee both before and during the periods of elevated AN concentrations on both days, and examination of these filters with the scanning electron microscope-energy dispersive X-ray analyzer (SEM-EDX) disclosed a large fraction of the particles on the filter that were typically of plume origin, i.e., with spherical shape and with sulfur as the predominant emitting element. In Figures 18 and 19 are shown the SEM-EDX analyses for some of these filter samples. These analyses were discussed earlier in this report. The finding of plume-typical particles in supposedly non-plume-exposed filters prompted an examination of the analysis record from Hay Coulee for evidence of plume exposure. Table 7 is a compilation of the pertinent information. We have listed all times when the AN concentration increased to at least double the level before and after. Episodes that, in our judgement, represented plume

exposure are indicated by a "P" in the left-hand column. Any examples of steady AN concentration readings were interpreted as being due to natural causes not related to the plume; this kind of variation in AN concentration is common. Plume exposure was judged to have occurred when changes were large in comparison to the background, were abrupt, and were individually of short duration. On this basis, Hay Coulee seems to have experienced plume exposure 21 different times for a total of about 30 hours out of 340 hours of observation from 1300 MDT, 20 August to 1700 MDT, 3 September 1977. Cloud condensation nuclei (CCN) and ice nuclei (IN) concentrations and light scattering (b_{scat}) are also listed in Table 7 whenever measurements were taken during an episode of elevated AN concentration; in addition, for comparison we have included many examples of CCN, IN, and b_{scat} levels when the AN concentrations were normal background. These have been discussed in another part of this report.

Figure 23 shows the record of AN and CCN concentrations at Hay Coulee on 23 August 1977, during an unmistakable plume strike from 0828 to 0845 MDT, a lesser exposure from about 1000 to 1010 MDT, and for the following time beginning at 1040 MDT, when there was no plume exposure, but the AN concentration reached a maximum of 2.8×10^4 cm^{-3}. During exposure, the AN concentration reached 4.8×10^4 μm^{-3}, the IN was offscale on the high side, and the patchy nature of the plume is indicated by the fact that, between pulses, the AN concentration fell almost to normal background levels. Figure 23 also shows the record AN measurements made with the research aircraft over Hay Coulee, both within and outside of the plume. These measurements are entirely consistent with, and supportive of, the measurements at the mobile laboratory in Hay Coulee.

10. Conclusions

The secondary particles found in the power plant plume with $r > 0.5$ μm are composed predominantly of nitrates from the oxidation of emitted NO and absorption of water. The particles of $r < 0.1$ μm were sulfates from the oxidation of SO_2; sulfate was also found absorbed on mineral particles. In terms of numbers the secondary particles in the plume were overwhelmingly sulfates. In the examples given, the rate of formation of secondary particles was about 10^{16} s^{-1}, with variation to greater or lesser production rates by a factor of roughly 5, depending upon power production level (i.e., coal consumption rate), coal S content, atmospheric temperature and solar energy input. In the example of 3 June 1978, the conversion rate of SO_2 to $SO_4^=$ particles of accumulation mode size was ~ 1 percent h^{-1}.

Plume dimensions as measured were compared to the predictions of theory; the predicted width was usually less than measured, but the predicted thickness was usually much larger than measured. Plume trajectories were found to be affected by underlying terrain. In one example the plume was diverted by as much as 20° to flow around a small mountain, in another example, the plume seemd to be ducted along a valley.

11. References

Abshire, N. L., Derr, V. E., McNice, G. T. Pueschel, R. F. and Van Valin, C. C. (1978) Aerosol characterization at Colstrip, Montana, spring and fall, 1975. EPA-600/3-78-021, pp. 291-321.

Barrett, E. W., Parungo, F. P. and Pueschel, R. F. (1979) Cloud modification by urban pollution: a physical demonstration. Meteorol. Rdsch. 32, 136-149.

Bigg, E. K., Mossop, S. C., Meade, R. T. and Thorndike, N.S.C. (1963) The measurement of ice nucleus concentrations by means of Millipore filters. J. Appl. Meteorol. 2, 266-269.

Bigg, E. K. Ono, A. and Williams, J. A. (1974) Chemical tests for individual submicron aerosol particles. Atmospheric Environment 8, 1-13.

Brighton, P. W. M. (1978) Strongly stratified flow past three-dimensional obstacles. Q. Jl. R. Met. Soc. 104, pp. 289-307.

Calvert, J. G. (1976) Test of the theory of ozone generation in Los Angeles atmosphere. Envir. Sci. Technol. 10, 248-256.

Clark, W. E. and Whitby, K. T. (1975) Measurements of aerosols produced by the photochemical oxidation of SO_2 in air. J. Colloid Interface Sci. 51, 477-490.

Friedlander, S. K. (1978) A review of the dynamics of sulfate containing aerosols. Atmospheric Environment 12, 187-195.

Gordon, C. C., Tourangeau, P. C. and Rice, P. M. (1978) Investigation of the impact of coal-fired power plant emissions upon the disease/health/growth characteristics of Ponderosa Pine-Skunk bush ecosystems and grassland ecosystems in southeastern Montana, In: "The Bioenvironmental Impact of a Coal-Fired Power Plant, Third Interim Report, Colstrip, Montana, E. M. Preston and R. A. Lewis, eds., EPA-600/3-78-021, Feb. 1978.

Hidy, G. M. and Lilly, D. K. (1965) Solutions to the equations for the kinetics of coagulation, J. Colloid Sci., 20, 867-874.

Hobbs, P. V., Stith, J. L. and Radke, L. F. (1980) Cloud-active nuclei from coal-fired electric power plants and their interactions with clouds. J. Appl. Meteorol. 19, 439-451.

Hunt, J. C. R., Puttock, J. S. and Snyder, W. H. (1979) Turbulent diffusion from a point source in stratified and neutral flows around a three-dimensional hill - Part I. Diffusion equation analysis. Atmospheric Environment 13, 1227-1239.

Langer, G., Rosinski, J. and Edwards, C. P. (1967) A continuous ice nucleus counter and its application to tracking in the troposphere. J. Appl. Meteorol. 6, 114-128.

Mamane, Y. and de Pena, R. G. (1978) A quantitative method for the detection of individual submicrometer size sulfate particles. Atmospheric Environment 12, 69-82.

Mamane, Y. and Pueschel, R. F. (1979) Oxidation of SO_2 on the surface of fly ash particles under low relative humidity conditions. Geophys. Res. Lett. 6, 109-112.

Mamane, Y. and Pueschel, R. F. (1980) A method for the detection of individual nitrate particles. Atmospheric Environment 14, 629-639.

McMahon, T. A. and Denison, P. J. (1979) Empirical atmospheric deposition parameters - a survey. Atmospheric Environment 13, 571-585.

Parungo, F., Ackerman, E., Proulx, H. and Pueschel, R. (1978) Nucleation properties of fly ash in a coal-fired power plant plume. Atmospheric Environment 12, 920-935.

Parungo, F. P., Pueschel, R. F. and Wellman, D. L. (1980) Chemical characteristics of oil refinery plumes in Los Angeles. Atmospheric Environment 14, 509-522.

Pueschel, R. F. and Mamane, Y. (1979) Mechanisms and rates of formation of sulfur aerosols in power plant plumes. Sophia Conference on Long-Range Transport, Proceedings, Sophia, Bulgaria.

Pueschel, R. F., Schnell, R. C., Weickmann, H. K. and Wellman, D. L. (1979) Aerosol and ice nuclei measurements in the plume of the Homer City, Pa., power plant. Geophys. Res. Lett. 6, 371-374.

Reid, J. D. (1979) Studies of pollutant transport and turbulent dispersion over rugged mountainous terrain near Climax, Colorado. Atmospheric Environment 13, 23-28.

Schnell, R. C., Van Valin, C. C. and Pueschel, R. F. (1976) Atmospheric ice nuclei: no detectable effects from a coal-fired powerplant plume. Geophys. Res. Lett. 3, 657-660.

Turner, D. B. (1970) Workbook of atmospheric dispersion estimates. Public Health Service, 999-AP-26, 84 pp.

U.S. Geological Survey (1963) Hardin, Montana, 1:250,000 topographic map (NL 13-7).

Van Valin, C. C. and Pueschel, R. F. (1978) Atmospheric aerosol observations at Colstrip, MT. In: Proceedings of the 4th Joint Conference on Sensing of Environmental Pollutants, American Chemical Society, Washington, D.C., pp. 742-745.

Van Valin, C. C. and Pueschel, R. F. (1981) Fine particle formation and transport in the Colstrip, Montana, powerplant plume. Atmospheric Environment 15, 177-189.

Van Valin, C. C., Pueschel, R. F., and Parungo, F. P. (1980a) Sulfate and nitrate in plume aerosols from a powerplant near Colstrip, MT. In: Environmental and Climatic Impact of Coal Utilization (Edited by J. J. Singh and A. Deepak), Academic Press, New York, pp. 35-48.

Van Valin, C. C., Pueschel, R. F., Wellman, D. L., Abshire, N. L., Lerfald G. M. and McNice, G. T. (1979) Aerosol characterization in the vicinity of Colstrip, Montana. In: The Bioenvironmental Impact of a Coal-Fired Powerplant, Fourth Interim Report (Edited by E. M. Preston and T. L. Gullett), EPA 600/3-79-044, pp. 2-52.

Van Valin, C. C., Pueschel, R. F., Wellman, D. L. and Williams, G. M. (1980b) Plume and aerosol properties near Colstrip. In: The Bioenvironmental Impact of a Coal-Fired Power Plant, Fifth Interim Report (Edited by E. M. Preston and D. W. O'Guinn), EPA-600/3-80-052, pp. 20-48.

Whitby, K. T. (1978) The physical characteristics of sulfur aerosols. Atmospheric Environment 12, 135-159.

Whitby, K. T., Cantrell, B. K. and Kittleson, D. B. (1978) Nuclei Formation Rates in a Coal-Fired Power Plant Plume, Atmospheric Environment 12, 313-321.

White, W. H. (1977) NO_x - O_3 photochemistry in power plant plumes: comparison of theory with observation. Envir. Sci. Technol. 11, 995-1000.